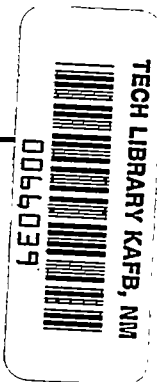


NACA TN 3263 1956



NATIONAL ADVISORY COMMITTEE FOR AERONAUTICS

TECHNICAL NOTE 3263

LIFT AND MOMENT EQUATIONS FOR OSCILLATING AIRFOILS

IN AN INFINITE UNSTAGGERED CASCADE

By Alexander Mendelson and Robert W. Carroll

Lewis Flight Propulsion Laboratory
Cleveland, Ohio



Washington

October 1954

AFM-C
TECHNICAL LIBRARY
AFL 2311

ERRATA

NACA TN 3263

LIFT AND MOMENT EQUATIONS FOR OSCILLATING AIRFOILS
IN AN INFINITE UNSTAGGERED CASCADE

By Alexander Mendelson and Robert W. Carroll

October 1954

2854

Page 8: Replace formula for C by the following equation:

$$C = \kappa \ln \frac{\epsilon^2 - 1}{\epsilon^2} + 1 + \frac{1 - \tau^{1/2}}{\tau^{1/2}} \frac{F(1/2, \kappa; \kappa + 1/2; 1/\tau)}{F(-1/2, \kappa; \kappa + 1/2; 1/\tau)}$$

Page 20: Line 13 should read "making use of equation (B11), to become".

Page 20: Unnumbered equation preceding equation (B25): Under the first integral (limits 1 to ϵ), the quantity $(\epsilon + \eta)^{\kappa-1}$ should be $(\epsilon - \eta)^{\kappa-1}$. Under the second integral (limits -1 to 1), the quantity $(\epsilon - \eta)^{m-1}$ should be $(\epsilon + \eta)^{m-1}$.

Page 20: Equation (B25) should be

$$\kappa \equiv \frac{ik}{2\lambda} + m$$

Page 24, equation (B40): The log factor of I_2 should be:

$$\log \frac{\epsilon + \mu}{\epsilon - \mu} \frac{d\mu}{\eta - \mu} d\eta$$



NATIONAL ADVISORY COMMITTEE FOR AERONAUTICS

TECHNICAL NOTE 3263

LIFT AND MOMENT EQUATIONS FOR OSCILLATING AIRFOILS

IN AN INFINITE UNSTAGGERED CASCADE

By Alexander Mendelson and Robert W. Carroll

SUMMARY

Exact equations are derived for the oscillatory aerodynamic forces acting in an unstaggered cascade of airfoils fluttering in potential flow. Aerodynamic coefficients similar to those of the isolated airfoil are obtained as functions of the cascade geometry and the phasing between successive blades; the phasings considered are zero, 90° , and 180° . It is shown that 90° is a special case of 180° phasing. These aerodynamic coefficients are plotted for the special case when all the airfoils are vibrating in bending in phase (360° phasing). It is shown that the effect of cascading for this case is to reduce greatly the aerodynamic damping.

INTRODUCTION

The flutter of airfoils in a cascade has until recently been primarily of academic interest. However, the widespread use of compressors and turbines in current aircraft power plants has given the problem significance. Compressor blades, in particular, are susceptible to vibrations, and some of these vibrations have been attributed to flutter.

The problem of the flutter of a compressor or turbine blade differs from that of an isolated airplane wing in at least two ways. It is necessary to consider, first, the effect of centrifugal force; and, second, the effect of cascading. The effect of centrifugal force can be taken into account with sufficient accuracy by applying the appropriate centrifugal force correction to the fundamental bending frequency (ref. 1). The effect of cascading is much more difficult to evaluate, however, since it is necessary to take into account the interference effect between the blades, which obviously depends on the cascade geometry. Two new geometric variables must therefore be introduced; namely, the spacing between blades and the stagger angle. In addition, since flutter is a time-varying phenomenon, another parameter must be introduced to take account of the phasing between the motions of the different blades of the cascade.

2854

CO-1

The problem of flutter of compressor blades is first simplified by assuming an infinite cascade of airfoils. A first step in a flutter analysis of such a cascade of airfoils is to determine the oscillatory aerodynamic forces and moments acting on the cascade. Most recorded cases of compressor blade flutter indicate the occurrence of such flutter at high aerodynamic loading, where the blade stalls and flow separation occurs, and it would be desirable to solve the problem for this case. However, no general methods for calculating aerodynamic forces in nonpotential flow are available. It is therefore necessary, as a first approach, to consider the case in potential flow at low angles of attack. The effect of flow separation at stall can then be taken into account separately, for instance, by the introduction of aerodynamic time lags (refs. 2 and 3) or other mechanisms which may prove useful. The object of this paper is to present solutions for several special cases of the oscillatory aerodynamic forces and moments acting on an infinite cascade of airfoils in potential flow.

The first derivation of oscillatory forces in a cascade was made in reference 4. The effect of the wind-tunnel walls on a fluttering isolated airfoil was determined approximately. This is equivalent to the special case of an infinite cascade without stagger, with adjacent blades being 180° out of phase. The integral equation for the problem was set up and an approximate solution obtained by replacing the kernel with a simple polynomial. The results are not applicable for spacing-to-chord ratios of less than 1. The same problem was solved rigorously in reference 5 and in reference 6 by different methods. The results are obtained in the form of doubly infinite series of Jacobian elliptic functions.

Another special case was treated in reference 7. A cascade with stagger with all the blades vibrating in phase is considered. The method is similar to that used in reference 8 for the isolated airfoil. The form in which the final results are presented cannot be easily used for numerical calculations. More recently, the general integral equation for a cascade with stagger and prescribed phasing was set up by Sisto (ref. 9). Approximate numerical solutions were then obtained for several cases of zero stagger. The method used is similar to that of reference 4.

The present paper attempts to fill some of the gaps left by the previously mentioned investigations. A solution is obtained for the case of zero stagger with the blades either 180° out of phase (considered in ref. 6), 90° out of phase, or in phase. The last two cases can be handled approximately by the method of reference 9. The present paper presents an exact solution. Furthermore, the results are obtained in a form which allows a solution in a simple straightforward manner on a desk calculator, the final results being presented in the form of aerodynamic coefficients which can be calculated in a stepwise manner by the use of a set of recurrence formulas.

AERODYNAMIC LIFT AND MOMENT

The analysis of the oscillatory forces and moments acting on a cascade of airfoils is made using the classical methods. In the beginning, the cascade is assumed to be of infinite extent with arbitrary spacing and stagger, as shown in figure 1. The problem is later specialized to the case of zero stagger. The airfoils are assumed to be thin and performing small oscillations in a potential, incompressible, ideal air-stream. The airfoils and their wakes are replaced by surfaces of discontinuity (vortex sheets), the interaction between the vortices being neglected. Each airfoil is performing both bending and torsional oscillations, two adjacent airfoils being out of phase by a prescribed amount.

Under these conditions Euler's equations of motion are first linearized and then solved for the pressure distribution over the airfoils. The Biot-Savart theorem giving the induced velocity at any point on the airfoil due to the vortex field must also be used to obtain a solution. Once the pressure distribution is known the aerodynamic lift and moment acting on the airfoil can be obtained by integration. The complete solution is given in appendix B. The final equations and results will be given here.

General case. - The aerodynamic lift and moment acting on an unstaggered cascade as obtained in the manner outlined can be expressed in a form similar to that given in reference 10 for the isolated airfoil.

$$L = \pi \rho b^3 \omega^2 \left\{ L_h \frac{h}{b} + \left[L_\alpha - \left(\frac{1}{2} + a \right) L_h \right] \alpha \right\}$$

$$M = \pi \rho b^4 \omega^2 \left\{ \left[M_h - \left(\frac{1}{2} + a \right) L_h \right] \frac{h}{b} + \left[M_\alpha - \left(\frac{1}{2} + a \right) (L_\alpha + M_h) + \left(\frac{1}{2} + a \right)^2 L_h \right] \alpha \right\}$$

where (all symbols are defined in appendix A)

- a elastic axis position as fraction of semichord b , measured from midchord, positive toward trailing edge
- b semichord
- h bending deflection, positive downward
- α torsional deflection about elastic axis, positive for increasing angle of attack
- ρ mass density of air
- ω circular flutter frequency

2854

CO-1 back

The aerodynamic coefficients L_h , L_α , M_h , M_α are functions of the following parameters:

k reduced frequency, $\omega b/V$

$2\pi m$ phase angle between adjacent blades; $m = 0, 1/2, 1/4$

λ cascade geometric parameter given by $\lambda \equiv \pi/s$

For the isolated airfoil these coefficients are functions of only the reduced frequency k . For convenience, the following additional parameters are used:

$$\sigma \equiv \coth \frac{\lambda}{2}$$

$$\epsilon \equiv \coth \lambda$$

$$\tau \equiv \left(\frac{\epsilon+1}{\epsilon-1} \right)^2$$

$$\pi \equiv \frac{\tau-1}{\tau}$$

$$\kappa \equiv \frac{ik}{2\lambda} + m$$

where

s spacing in units of semichord

V free-stream velocity

The following scheme, as outlined in appendix C, is now used to calculate the aerodynamic coefficients: Let

$$a_0 = 0; a_1 = 1; b_0 = 1$$

$$a_{j+1} \equiv \frac{1}{j} \left[(j-2)a_{j-1} - 2ma_j \right] \quad j \geq 1$$

$$b_j = b_{j-1} + a_{j+1}$$

$$c_j = \sigma^{-j} \sum_{i=0}^{\infty} \frac{b_i b_{i+j}}{\sigma^{2i}} = c_{-j} \quad j \geq 0$$

$$d_j = \sum_{i=0}^{\infty} \frac{c_{j+1+2i} + c_{j-1-2i}}{(2i+1)\sigma^{2i}} = d_{-j} \quad j \geq 0$$

$$e_j = \sum_{i=0}^{\infty} \frac{d_{j+1+2i} + d_{j-1-2i}}{(2i+1)\sigma^{2i}} = e_{-j} \quad j \geq 0$$

$$f_j = c_j + 2 \sum_{i=j}^{\infty} c_{i+1}$$

$$C_j = (-1)^j (c_{j-1} + 2c_j + c_{j+1})f_j$$

$$D_j = (-1)^j (d_{j-1} + 2d_j + d_{j+1})f_j$$

$$E_j = (-1)^j (e_{j-1} + 2e_j + e_{j+1})f_j$$

$$F_j = (-1)^j (d_{j-1} + 2d_j + d_{j+1}) \sum_{i=0}^{j-1} (d_{j-2i} + d_{j-1-2i})$$

$$G_j = (-1)^j (d_{j-1} + 2d_j + d_{j+1}) \sum_{i=0}^{j-1} (e_{j-2i} + e_{j-1-2i})$$

$$A_0 = 1$$

$$A_{j+1} = \frac{2j+1}{2j+4} A_j$$

$\Gamma(z) \equiv$ gamma function of argument z

$$(\chi, j) \equiv \chi(\chi+1)(\chi+2) \cdots (\chi+j-1) = \frac{\Gamma(\chi+j)}{\Gamma(\chi)}$$

$$F(1/2, \chi; \chi + 1/2 + q; 1/\tau) \equiv \sum_{i=0}^{\infty} \frac{(1/2, i)(\chi, i)}{(\chi + 1/2 + q, i)(1, i)} \tau^{-i}$$

is the ordinary hypergeometric function.

2854

$$B_p = \frac{(1+m, p)}{p!} \sum_{q=0}^p (-1)^q \frac{(\alpha, q)(-p, q)}{(\alpha+1/2, q)(1+m, q)} (\tau T)^{-q} F(1/2, \alpha; \alpha + 1/2 + q; 1/\tau)$$

$$R_1 = 1 + \frac{\alpha-m}{2} T \tau^{1/2-m} \frac{\Gamma(\alpha)\Gamma(1/2)}{\Gamma(\alpha+1/2)} \sum_{p=0}^{\infty} A_p B_p T^p$$

$$R_2 = 1 + \frac{(\alpha-m)^2}{2} T \tau^{1/2-m} \frac{\Gamma(\alpha)\Gamma(1/2)}{\Gamma(\alpha+1/2)} \sum_{j=1}^{\infty} \sum_{p=0}^{\infty} \frac{1}{j} A_{j+p} B_p T^{j+p}$$

$$R_3 = 1 + \frac{(\alpha-m)^3}{4} T \tau^{1/2-m} \frac{\Gamma(\alpha)\Gamma(1/2)}{\Gamma(\alpha+1/2)} \sum_{i=1}^{\infty} \sum_{j=1}^{\infty} \sum_{p=0}^{\infty} \frac{1}{ij} A_{i+j+p} B_p T^{i+j+p}$$

$$P_1(\lambda, m) = \frac{8e}{\lambda \sigma^2} \left(\frac{1}{2} C_0 + \sum_{j=1}^{\infty} C_j \right)$$

$$P_2(\lambda, m) = \frac{8e}{\lambda^2 \sigma^3} \left(\frac{1}{2} D_0 + \sum_{j=1}^{\infty} D_j \right)$$

$$P_3(\lambda, m) = -\frac{8e}{\lambda^3 \sigma^4} \sum_{j=1}^{\infty} F_j$$

$$P_4(\lambda, m) = +\frac{4e}{\lambda^3 \sigma^4} \left(\frac{1}{2} E_0 + \sum_{j=1}^{\infty} E_j \right)$$

$$P_5(\lambda, m) = -\frac{4e}{\lambda^4 \sigma^5} \sum_{j=1}^{\infty} G_j$$

$$C(k, \lambda, m) = -ik + \frac{2ik + R_2}{R_1}$$

$$D(k, \lambda, m) = ikC - \frac{k^2}{2} - \frac{2ik - 2k^2 + R_3}{R_1}$$

The aerodynamic coefficients can now be obtained as follows:

$$L_h = P_2 - \frac{i}{k} P_1 C$$

$$L_\alpha = \frac{1}{2} L_h + P_3 - \frac{i}{k} P_2 (1 + C) - \frac{P_1}{k^2} C$$

$$M_h = \left(\frac{1}{2} + \frac{i}{k} \right) L_h - P_4 + \frac{P_1}{k^2} D$$

$$M_\alpha = \frac{1}{2} \left(L_\alpha + M_h - \frac{1}{2} L_h \right) + \frac{1}{k^2} L_h - P_5 + \frac{i}{k} (P_3 + P_4) + \frac{P_2}{k^2} (C + D) - \frac{i}{k^3} P_1 D$$

The geometric parameters $\lambda, \epsilon, \sigma, \tau, \Gamma$ are functions of the spacing and have been tabulated in table I for different spacings.

The quantities a_j and b_j are functions of only the phasing m . The first 20 values of b_j have been tabulated in table II for values of m equal to 0 and $1/2$. It is to be noted that for $m = 0$, b_j is equal to 1 for all j .

In the equations for c_j, d_j , and e_j , the index j never takes on negative values. The quantities c_{-j}, d_{-j}, e_{-j} must always be obtained by calculating c_j, d_j , and e_j .

The P_1, P_2, P_3, P_4 , and P_5 are functions of the cascade geometric parameter λ and the phasing between blades m . The functions C and D are functions of λ, m , and the reduced frequency k . It is shown in appendix B that the case $m = 1/4$ (90° phasing) reduces to the case $m = 1/2$ (180° phasing) with twice the spacing. For the case of an isolated airfoil, the functions reduce as follows:

$$\begin{aligned} s &\rightarrow \infty & P_3 &\rightarrow 0 \\ \lambda &\rightarrow 0 & P_4 &\rightarrow 1/2 \\ P_1 &\rightarrow 2 & P_5 &\rightarrow 1/8 \\ P_2 &\rightarrow 1 \end{aligned}$$

$$C(\lambda, m, k) \rightarrow C(k) \text{ Theodorsen's function}$$

$$D(\lambda, m, k) \rightarrow -C(k) - \frac{ik}{2} \left[1 - C(k) \right] + \frac{k^2}{4}$$

2854

The coefficients L_h , L_u , M_h , and M_u then reduce identically to those of the isolated airfoil as given in reference 10.

The values of A_j are independent of geometry or phasing. The first 30 values are tabulated in table III.

Special case, $m = 0$: For the case of all the blades vibrating in phase ($m=0$), a few simplifications can be made.

$$a_j = 0$$

$$b_j = 1 \text{ for all } j$$

$$c_j = \frac{\sigma^2}{\sigma^2 - 1} \sigma^{-j}$$

$$f_j = \frac{\sigma^2}{(\sigma - 1)^2} \sigma^{-j}$$

$$P_1 = \frac{2}{\lambda(\epsilon - 1)}$$

$$P_2 = \frac{\epsilon}{\lambda^2(\epsilon - 1)} \ln \frac{\epsilon^2}{\epsilon^2 - 1}$$

$$C = \kappa \ln \frac{\epsilon^2 - 1}{\epsilon^2} + \frac{1 - \left(\frac{\tau - 1/2}{\kappa + 1/2} \right)^{\kappa} F(1/2, \kappa; \kappa + 1/2; 1/\tau)}{\tau^{1/2} F(-1/2, \kappa; \kappa + 1/2; 1/\tau)}$$

For this case, therefore, the bending coefficient L_h is obtained in closed form. The preceding results can be obtained by summing the series for the appropriate quantities or by integrating I_1 , I_2 , I_6 , and I_7 of appendix B directly for $m = 0$.

APPLICATION AND RESULTS

As an example, the case in which all the blades are vibrating in phase ($m=0$) will be considered. Experimental data on compressors indicate that the only important type of vibration occurring is one of pure bending. For this case, then, the only aerodynamic coefficient that need be considered is L_h .

The functions P_1 and P_2 are plotted in figure 2 against the cascade geometry parameter λ . The real and imaginary parts of the circulation function C are plotted in figure 3. It is to be noted that C is a function of both the spacing and the reduced frequency, whereas the P functions are independent of the reduced frequency.

In figure 3, over the range of reduced frequencies from zero to 0.6 and spacings $s = 1.67$ to 3.33 (this corresponds to solidities of 0.83 to 1.67), the real part of the circulation function C is independent of reduced frequency for practical purposes, whereas the imaginary part of C varies linearly with reduced frequency.

With the P functions and the circulation function C available, the aerodynamic bending coefficient L_h was computed and plotted in figure 4. The values for the isolated airfoil are also plotted on this figure. It is to be noted that L_h (as well as the other coefficients) is complex. The real part of L_h is in phase with the displacement and can do no work; the imaginary part is in phase with the velocity and corresponds to the damping component and can do work. Whether this system is stable therefore depends on the sign of the out-of-phase component or imaginary part of L_h . The real part of L_h is practically independent of reduced frequency and varies only slightly with spacing in the range considered. The imaginary part of L_h , however, varies appreciably both with reduced frequency and spacing. This is further illustrated in figure 5, where the coefficient L_h has been plotted against spacing for a reduced frequency of 0.4. The results of figure 4 agree well with those of reference 9 for a spacing s of 2.0, which is the only one considered there. Some of the data from that reference are plotted in the figure.

Since the imaginary part, or out-of-phase component of L_h , corresponds to the aerodynamic damping, figure 4 shows clearly that the effect of cascading is to reduce greatly the aerodynamic damping when the blades are vibrating in phase. For example, at a reduced frequency k of 0.4 and spacing s of 2 (solidity of 1), the aerodynamic damping is approximately one-half the value for the isolated airfoil. At a reduced frequency of 0.1, the damping is reduced to almost one-third the isolated airfoil value. The higher the solidity, the lower the aerodynamic damping becomes. However, for this particular phasing (all the blades vibrating in phase), the damping never actually goes to zero in pure bending except in the limit of infinite solidity.

CONCLUDING REMARKS

The equations for the oscillatory aerodynamic forces acting in several cases on a cascade of airfoils in potential flow are derived. The aerodynamic bending coefficient is calculated and plotted for the case

2854

2-8

where all the blades are vibrating in phase. For this case, the effect of cascading is to reduce greatly the aerodynamic damping force.

The results of this investigation can be used in the study of stall flutter phenomena in a cascade in a manner similar to the use of the classical flutter theory of the isolated airfoil for the stall flutter of the isolated airfoil. Aerodynamic time lags can be introduced into or characteristic times (ref. 2) can be deduced from the aerodynamic lift and moment equations. The linear part of the blade characteristic (ref. 11) is directly obtainable, and the nonlinear part, if known, might be treated by the methods of reference 2. The general usefulness of this approach, for both the isolated airfoil and a cascade, must, however, still be determined.

Lewis Flight Propulsion Laboratory
National Advisory Committee for Aeronautics
Cleveland, Ohio, July 16, 1954

APPENDIX A

SYMBOLS

The following symbols are used in this report:

a	elastic axis position, measured from midchord, as a fraction of semichord b , positive toward trailing edge
$A_j, B_j, a_j, b_j,$ c_j, d_j, e_j	coefficients in recurrence formulas given in text
b	semichord
$C(k, \lambda, m)$ $D(k, \lambda, m)$	functions defined in text
$C_j, D_j, E_j,$ F_j, G_j	coefficients used in evaluating integrals, given in text
e	base of natural logarithms
$f(t), f(\eta), g(\mu)$	functions of indicated variables
h	bending displacement of airfoil, positive downward
i	$\sqrt{-1}$
$I_1, I_2, I_3, I_4,$ I_5, I_6, I_7, I_8	integrals defined by eqs. (B40) and (B41)
k	reduced frequency, $\omega b/V$
L	lift per unit span
L_h, L_α	aerodynamic coefficients in lift equation, defined in text
M	moment about elastic axis
M_h, M_α	aerodynamic coefficients in moment equations, defined in text
m	phase angle lag between any two adjacent blades, as fraction of 2π radians, $\delta/2\pi$, appendix B

2854

CQ-2 back

$P_1, P_2, P_3,$ P_4, P_5	functions defined in text
p'	pressure at any point on airfoil, function of time
Δp	amplitude of pressure difference
$\Delta p'$	pressure difference at a point on airfoil, $p_u' - p_l'$, function of time
s	spacing between blades in units of semichord b
T	geometric parameter defined by $\frac{\tau-1}{\tau}$
t	time
u	local velocity component in free-stream direction
V	free-stream velocity
v	local velocity component perpendicular to free-stream direction
x, x_1	coordinate in free-stream direction in units of semichord
y	coordinate perpendicular to free-stream direction in units of semichord
α	angular displacement of airfoil
β	stagger angle
Γ	total circulation about airfoil
γ	vorticity distribution for reference airfoil
γ_w	vorticity distribution in wake of reference airfoil
δ	phase angle between two adjacent blades
ε	geometric parameter defined by $\varepsilon \equiv \coth \lambda$
ζ, ζ', ν η, η_1, μ	transformed variables of integration defined in appen- dixes C and D
x	$\frac{ik}{2\lambda} + m$

λ	geometric parameter defined by $\frac{\pi}{s} e^{i\beta}$
ρ	air density
σ	geometric parameter defined by $\sigma \equiv \coth \frac{\lambda}{2}$
τ	geometric parameter defined by $\tau \equiv \left(\frac{e+1}{e-1} \right)^2$
ϕ	velocity potential
ω	circular frequency of oscillation

Subscripts:

i, j, n, p, q	summation indices
u	upper surface of airfoil
l	lower surface of airfoil

The subscript n is used also to indicate the n^{th} airfoil

APPENDIX B

LIFT AND MOMENT EQUATIONS

General Theory

The analysis of the oscillating airfoil of infinite aspect ratio in a cascade proceeds along classical lines. The airfoil is assumed to be of small camber and thickness and performing infinitesimal oscillations in an incompressible ideal fluid moving at a velocity V at infinity.

The airfoil and its wake are replaced by a surface of discontinuity or vortex sheet of strength γ' over the airfoil and γ'_w in the wake. This surface of discontinuity is assumed to lie in a horizontal plane parallel to the direction of flow. The vertical displacement due to the interaction between vortices of this sheet is neglected, this displacement being assumed small compared with the horizontal motion. The assumption of small perturbations to the free-stream velocity permits the linearization of Euler's equations and, with the introduction of a velocity potential, Bernoulli's equation for nonsteady incompressible flow is obtained. The derivation is given here in detail for completeness.

Euler's equations for two-dimensional flow can be written

$$\left. \begin{aligned} \frac{\partial}{\partial t} (V+u) + (V+u) \frac{\partial}{\partial x} (V+u) + v \frac{\partial}{\partial y} (V+u) &= -\frac{1}{\rho} \frac{\partial p'}{\partial x} \\ \frac{\partial v}{\partial t} + (V+u) \frac{\partial v}{\partial x} + v \frac{\partial v}{\partial y} &= -\frac{1}{\rho} \frac{\partial p'}{\partial y} \end{aligned} \right\} \quad (B1)$$

Considering only first-order terms and realizing V is a constant give the linearized Euler equations as

$$\left. \begin{aligned} \frac{\partial u}{\partial t} + V \frac{\partial u}{\partial x} &= -\frac{1}{\rho} \frac{\partial p'}{\partial x} \\ \frac{\partial v}{\partial t} + V \frac{\partial v}{\partial x} &= -\frac{1}{\rho} \frac{\partial p'}{\partial y} \end{aligned} \right\} \quad (B2)$$

The velocity potential ϕ is now introduced:

$$\left. \begin{aligned} u &= \frac{\partial \phi}{\partial x} \\ v &= \frac{\partial \phi}{\partial y} \end{aligned} \right\} \quad (B3)$$

Equation (B2) can now be written

$$\left. \begin{aligned} \frac{\partial}{\partial x} \left(\frac{\partial \Phi}{\partial t} \right) + V \frac{\partial}{\partial x} \left(\frac{\partial \Phi}{\partial x} \right) &= - \frac{1}{\rho} \frac{\partial p'}{\partial x} \\ \frac{\partial}{\partial y} \left(\frac{\partial \Phi}{\partial t} \right) + V \frac{\partial}{\partial y} \left(\frac{\partial \Phi}{\partial x} \right) &= - \frac{1}{\rho} \frac{\partial p'}{\partial y} \end{aligned} \right\} \quad (B4)$$

which leads directly to Bernoulli's equation for nonsteady motion

$$\frac{\partial \Phi}{\partial t} + V \frac{\partial \Phi}{\partial x} + \frac{1}{\rho} p' = f(t) \quad (B5)$$

The airfoil and its wake are now replaced by a vortex sheet of strength γ' on the airfoil and γ'_w in the wake. The difference between the velocities of upper and lower surfaces of the vortex sheet is therefore γ' or γ'_w . For a point on the airfoil, therefore,

$$\frac{\partial \Phi_u}{\partial x} - \frac{\partial \Phi_l}{\partial x} = \gamma'$$

which upon integration gives

$$\Phi_u - \Phi_l = b \int_{-1}^x \gamma' dx_1 \quad (B6)$$

Equations (B5) and (B6) then give

$$\Delta p' \equiv p_u' - p_l' = -\rho \left(V \gamma' + b \frac{\partial}{\partial t} \int_{-1}^x \gamma' dx_1 \right) \quad (B7)$$

Continuity of pressure in the wake requires that Δp be zero there, and equation (B7) becomes, for the wake,

$$\gamma'_w + \frac{b}{V} \frac{\partial}{\partial t} \int_1^x \gamma'_w dx_1 = - \frac{b}{V} \frac{\partial \Gamma'}{\partial t} \quad (B8)$$

where

$$\Gamma' \equiv \int_{-1}^1 \gamma' dx_1 \quad (B9)$$

The assumption of simple harmonic motion will now be made, so that

$$\left. \begin{aligned} y' &= ye^{i\omega t} \\ v' &= ve^{i\omega t} \\ \gamma' &= \gamma e^{i\omega t} \\ \gamma_w' &= \gamma_w e^{i\omega t} \\ \Gamma' &= \Gamma e^{i\omega t} = e^{i\omega t} \int_{-1}^1 \gamma dx \\ \Delta p' &= \Delta p e^{i\omega t} \end{aligned} \right\} \quad (B10)$$

Equation (B8) now becomes

$$\gamma_w + ik \int_1^x \gamma_w dx_1 = -ik\Gamma \quad (B8a)$$

Equation (B8a) is a simple nonhomogeneous integral equation with the kernel equal to 1. Its solution is

$$\gamma_w = -ik\Gamma e^{-ik(x-1)} \quad (B11)$$

Equation (B11) gives the vorticity distribution in the wake as a function of the total circulation around the airfoil. It can also be obtained from the condition that the total circulation around the system comprising the airfoil and the wake must equal zero.

With the use of equation (B7) the pressure distribution over the airfoil can now be written in the following form:

$$-\frac{\Delta p}{\rho V} = \gamma + ik \int_{-1}^x \gamma dx_1 \quad (B12)$$

The lift and moment about the elastic axis can be found by integrating the pressure distribution as follows:

$$\left. \begin{aligned} L &= -\rho V b \int_{-1}^1 \gamma dx - i \rho V b k \int_{-1}^1 \int_{-1}^x \gamma dx_1 dx \\ M &= -\rho V b^2 \int_{-1}^1 \gamma(x-a) dx - i b^2 \rho V k \int_{-1}^1 (x-a) \int_{-1}^x \gamma dx_1 dx \end{aligned} \right\} (B13)$$

Vorticity Distribution in a Cascade

Consider an infinite cascade of airfoils of chord 2, stagger angle β , and spacing s as indicated in figure 1. The airfoils are replaced by vortex sheets, the vorticity of the n^{th} sheet being designated by use of a subscript n . The Biot-Savart theorem is applied to give the induced velocity at a point x on the reference airfoil due to an element of vorticity of strength γ_n located at the point $(x_1, ns \cos \beta)$.

$$dv_n = \frac{-\gamma_n(x - x_1)dx_1}{2\pi \left[(x - x_1)^2 + (ns \cos \beta)^2 \right]} \quad (B14)$$

Measuring from the y' axis, this can be written

$$-dv_n = -\frac{\gamma_n(x - x_1 - ns \sin \beta)dx_1}{2\pi \left[(ns \cos \beta)^2 + (x - x_1 - ns \sin \beta)^2 \right]} \quad (B14a)$$

Summing over all n and integrating from -1 to ∞ change equation (B14a) to

$$v(x) = -\frac{1}{2\pi} \int_{-1}^{\infty} \sum_{n=-\infty}^{\infty} \frac{\gamma_n(x - x_1 - ns \sin \beta)dx_1}{\left[ns \cos \beta + i(x - x_1 - ns \sin \beta) \right] \left[ns \cos \beta - i(x - x_1 - ns \sin \beta) \right]} \quad (B15)$$

The assumption is now made that any two adjacent blades are out of phase by an angle

$$\delta = 2\pi m \quad 0 \leq m \leq 1$$

2854

CQ-3

This angle is constant through the cascade. The vorticity distribution of the n^{th} blade is therefore out of phase with that of the reference blade at the origin by an angle

$$\delta_n = 2\pi mn$$

or

$$\gamma_n = \gamma e^{i2\pi mn} \quad (\text{B16})$$

where γ is the vorticity distribution for the reference blade. Substituting γ_n into equation (B15) results in

$$v(x) = -\frac{i}{4\pi} \int_{-1}^{\infty} \frac{\gamma(x_1)}{se^{-i\beta}} \sum_{n=-\infty}^{\infty} \frac{e^{i2\pi mn}}{i(x_1-x) - se^{-i\beta}} dx_1 + \frac{i}{4\pi} \int_{-1}^{\infty} \frac{\gamma(x_1)}{se^{i\beta}} \sum_{n=-\infty}^{\infty} \frac{e^{i2\pi mn}}{i(x-x_1) - se^{i\beta}} dx_1 \quad (\text{B17})$$

The infinite sums can be evaluated (see ref. 12).

$$\sum_{n=-\infty}^{\infty} \frac{e^{i2\pi mn}}{e^{i\beta}(x-x_1) - s} = i\pi \frac{e^{-\lambda(1-2m)(x-x_1)}}{\sinh \lambda(x-x_1)} \quad (\text{B18})$$

$$\lambda \equiv \frac{\pi}{s} e^{i\beta}$$

Substituting now equation (B18) into equation (B17) gives

$$v(x) = \frac{\lambda}{4\pi} \int_{-1}^{\infty} \frac{\gamma(x_1) e^{-\lambda(2m-1)(x-x_1)}}{\sinh \lambda(x_1-x)} dx_1 + \frac{\bar{\lambda}}{4\pi} \int_{-1}^{\infty} \frac{\gamma(x_1) e^{\bar{\lambda}(2m-1)(x_1-x)}}{\sinh \bar{\lambda}(x_1-x)} dx_1 \quad (\text{B19})$$

$$\bar{\lambda} = \frac{\pi}{s} e^{-i\beta}$$

It should be noted that although equation (B18) is not valid for $m = 0$, equation (B19) is valid for all m . Equation (B19) gives the induced velocity at a point on the airfoil due to the complete vortex field of the cascade. It reduces to the well-known equation for the

isolated airfoil when the spacing s goes to infinity. If use is made of the condition that the normal induced velocity must equal the normal component of the velocity of the airfoil, then equation (B19) gives the relation between the normal component of motion of the airfoil and the vorticity distribution. The problem then becomes one of solving equation (B19) for the vorticity distribution as a function of the airfoil motion. Once the vorticity distribution is known, the pressure distribution can be calculated from equation (B12).

The solution of the general equation (B19) will not be attempted here. Instead, several special cases of zero stagger will be considered. For this case, $\beta = 0$, $\lambda = \bar{\lambda} = \pi/s$, and equation (B19) reduces to

$$v(x) = \frac{\lambda}{2\pi} \int_{-1}^{\infty} \frac{\gamma(x_1) \cosh \lambda(1-2m)(x_1-x)}{\sinh \lambda(x_1-x)} dx_1 \quad (B20)$$

Equation (B20) will now be solved for the following three values of m :

- $m = 0$ all the blades are in phase
- $m = \frac{1}{2}$ adjacent blades are 180° out of phase
- $m = \frac{1}{4}$ adjacent blades are 90° out of phase

For $m = 0$,

$$\left. \begin{aligned} v(x) &= \frac{\lambda}{2\pi} \int_{-1}^{\infty} \gamma(x_1) \frac{\cosh \lambda(x_1-x)}{\sinh \lambda(x_1-x)} dx_1 \\ &= \frac{\lambda}{2\pi} \int_{-1}^{\infty} \gamma(x_1) \frac{e^{\lambda(x_1-x)}}{\sinh \lambda(x_1-x)} dx_1 \end{aligned} \right\} \quad (B21)$$

The second equation follows from Kelvin's theorem, since $\int_{-1}^{\infty} \gamma(x_1) dx_1 = 0$. For $m = 1/2$,

$$v(x) = \frac{\lambda}{2\pi} \int_{-1}^{\infty} \frac{\gamma(x_1)}{\sinh \lambda(x_1-x)} dx_1 \quad (B22)$$

2854

CQ-3 back

For $m = 1/4$,

$$\begin{aligned}
 v(x) &= \frac{\lambda}{2\pi} \int_{-1}^{\infty} r(x_1) \frac{\cosh \frac{\lambda}{2}(x_1-x)}{\sinh \lambda(x_1-x)} dx_1 \\
 &= \frac{\lambda/2}{2\pi} \int_{-1}^{\infty} \frac{r(x_1)}{\sinh \frac{\lambda}{2}(x_1-x)} dx_1 \quad (B23)
 \end{aligned}$$

The case for $m = 1/4$ therefore reduces to the case of $m = 1/2$ with twice the spacing. The same result can be obtained from purely physical considerations. Thus only equations (B21) and (B22) have to be solved.

In order to solve equations (B21) and (B22), a transformation of variables similar to that used in reference 6 will be made. Let

$$\left. \begin{aligned}
 \tanh \lambda x &\equiv \mu/\epsilon \\
 \tanh \lambda x_1 &\equiv \eta/\epsilon \\
 \tanh \lambda &\equiv 1/\epsilon
 \end{aligned} \right\} \quad (B24)$$

Equations (B21) and (B22) can then be written in terms of μ and η , making use of equation (B20), to become

$$\begin{aligned}
 v(\mu) \frac{(\epsilon-\mu)^{m-1}}{(\epsilon+\mu)^m} - i \frac{k\Gamma}{2\pi} e^{ik} \int_{-1}^{\epsilon} \frac{e^{(\epsilon+\eta)x-1}}{(\epsilon+\eta)^x} \frac{d\eta}{\mu-\eta} &= \frac{-1}{2\pi} \int_{-1}^1 \frac{r(\eta)(\epsilon-\eta)^m}{(\epsilon^2-\eta^2)(\epsilon-\eta)^{m-1}} \frac{d\eta}{\mu-\eta} \\
 x &\equiv \frac{ik}{2} + m \quad (B25)
 \end{aligned}$$

where m takes on the value of 0 or $1/2$. Or, more briefly,

$$g(\mu) = \frac{1}{2\pi} \int_{-1}^1 \frac{f(\eta)}{\mu-\eta} d\eta \quad (B26)$$

where $g(\mu)$ and $f(\eta)$ correspond to the appropriate parts of equation (B25).

Equation (B26) has an explicit solution for $f(\eta)$, first obtained in reference 13 and proven rigorously for the real domain in references 14 and 15. With the condition $f(1)$ finite, the solution is

$$f(\eta) = -\frac{2}{\pi} \sqrt{\frac{1-\eta}{1+\eta}} \int_{-1}^1 g(\mu) \sqrt{\frac{1+\mu}{1-\mu}} \frac{d\mu}{\eta-\mu} \quad (B27)$$

The solution of equation (B25) can now be written directly.

$$\frac{\gamma(\eta)}{e^{\frac{2}{2}-\eta^2}} = \frac{2}{\pi} \sqrt{\frac{1-\eta}{1+\eta}} \frac{(\epsilon+\eta)^{m-1}}{(\epsilon-\eta)^m} \left[\int_{-1}^1 v(\mu) \sqrt{\frac{1+\mu}{1-\mu}} \frac{(\epsilon-\mu)^{m-1}}{(\epsilon+\mu)^m} \frac{d\mu}{\eta-\mu} - \frac{ik\Gamma}{2\pi} e^{ik} \int_{-1}^1 \sqrt{\frac{1+\mu}{1-\mu}} \frac{1}{\eta-\mu} \int_1^\epsilon \frac{(\epsilon-\eta_1)^{\alpha-1}}{(\epsilon+\eta_1)^\alpha} \frac{d\eta_1}{\mu-\eta_1} d\mu \right] \quad (B28)$$

The second integral can be partly evaluated by reversing the order of integration:

$$\int_{-1}^1 \sqrt{\frac{1+\mu}{1-\mu}} \frac{d\mu}{(\eta-\mu)(\mu-\eta_1)} = \frac{\pi}{\eta_1-\eta} \sqrt{\frac{\eta_1+1}{\eta_1-1}} \quad (B29)$$

Substituting equation (B29) into equation (B28) results in

$$\frac{\gamma(\eta)}{e^{\frac{2}{2}-\eta^2}} = \frac{2}{\pi} \sqrt{\frac{1-\eta}{1+\eta}} \frac{(\epsilon+\eta)^{m-1}}{(\epsilon-\eta)^m} \left[\int_{-1}^1 v(\mu) \sqrt{\frac{1+\mu}{1-\mu}} \frac{(\epsilon-\mu)^{m-1}}{(\epsilon+\mu)^m} \frac{d\mu}{\eta-\mu} - \frac{ik\Gamma}{2} e^{ik} \int_1^\epsilon \frac{(\epsilon-\eta_1)^{\alpha-1}}{(\epsilon+\eta_1)^\alpha} \sqrt{\frac{\eta_1+1}{\eta_1-1}} \frac{d\eta_1}{\eta_1-\eta} \right] \quad (B30)$$

also

$$\Gamma = \frac{e}{\lambda} \int_{-1}^1 \frac{\gamma(\eta)}{e^{\frac{2}{2}-\eta^2}} d\eta \quad (B31)$$

Equation (B30) can be integrated as indicated in equation (B31) to obtain the total circulation around the airfoil Γ .

2854

$$\Gamma = \frac{\frac{2}{\pi} \frac{\epsilon}{\lambda} \int_{-1}^1 \sqrt{\frac{1-\eta}{1+\eta}} \frac{(\epsilon+\eta)^{m-1}}{(\epsilon-\eta)^m} \int_{-1}^1 v(\mu) \sqrt{\frac{1+\mu}{1-\mu}} \frac{(\epsilon-\mu)^{m-1}}{(\epsilon+\mu)^m} \frac{d\mu}{\eta-\mu} d\eta}{1 + \frac{i k e^{i k}}{\pi} \frac{\epsilon}{\lambda} \int_{-1}^1 \sqrt{\frac{1-\eta}{1+\eta}} \frac{(\epsilon+\eta)^{m-1}}{(\epsilon-\eta)^m} \int_{-1}^{\epsilon} \sqrt{\frac{\eta_1+1}{\eta_1-1}} \frac{(\epsilon-\eta_1)^{x-1}}{(\epsilon+\eta_1)^x} \frac{d\eta_1}{\eta_1-\eta} d\eta} \quad (B32)$$

Equations (B30) and (B32) give explicitly the vorticity distribution over the airfoil. With the vorticity distribution known, the pressure distribution and hence the lift and moment can now be calculated.

Lift and Moment on Airfoil in Cascade

Consider the airfoil shown in figure 6. The upward displacement at any time t of a point x on the airfoil is

$$y(x,t) = -h - b(x-a)\alpha \quad (B33)$$

The induced velocity $v(x)$ must satisfy the condition that the flow is everywhere tangential to the surface. If the induced velocity in the x -direction is small compared with free-stream velocity V , this condition leads to

$$\left. \begin{aligned} v(x) &= \left(V \frac{\partial y}{\partial x} + \frac{\partial y}{\partial t} \right) \\ &= -(h + V\alpha - ba\dot{\alpha} + b\dot{\alpha}x) \end{aligned} \right\} \quad (B34)$$

or, in the η coordinate,

$$v(\eta) = -(h + V\alpha - ba\dot{\alpha}) - \frac{b}{2\lambda} \dot{\alpha} \log \frac{\epsilon+\eta}{\epsilon-\eta} \quad (B35)$$

The lift and moment are given by

$$\left. \begin{aligned} L &= b \int_{-1}^1 \Delta p(x) dx = \int_{-b}^b \Delta p(\xi) d\xi \\ M &= b^2 \int_{-1}^1 \Delta p(x) (x-a) dx \end{aligned} \right\} \quad (B36)$$

Combining equations (B13), (B30), (B32), (B35), and (B36) and performing considerable algebraic manipulation, the lift and moment can be written in the following form:

$$\left. \begin{aligned}
 L &= \pi \rho b^3 \omega^2 \left\{ L_h \frac{h}{b} + \left[L_a - \left(\frac{1}{2} + a \right) L_h \right] \alpha \right\} \\
 M &= \pi \rho b^4 \omega^2 \left\{ \left[M_h - \left(\frac{1}{2} + a \right) L_h \right] \frac{h}{b} + \left[M_\alpha - \left(\frac{1}{2} + a \right) (L_\alpha + M_h) + \left(\frac{1}{2} + a \right)^2 L_h \right] \alpha \right\}
 \end{aligned} \right\} \tag{B37}$$

where

$$\left. \begin{aligned}
 L_h &\equiv P_2(\lambda, m) - \frac{i}{k} P_1(\lambda, m) C(k, \lambda, m) \\
 L_\alpha &\equiv \frac{1}{2} L_h + P_3(\lambda, m) - \frac{i}{k} P_2(\lambda, m) [1 + C(\lambda, m, k)] - \frac{P_1(\lambda, m)}{k^2} C(\lambda, m, k) \\
 M_h &\equiv \left(\frac{1}{2} + \frac{i}{k} \right) L_h - P_4(\lambda, m) + \frac{P_1(\lambda, m)}{k^2} D(\lambda, m, k) \\
 M_\alpha &\equiv \frac{1}{2} (L_\alpha + M_h - \frac{1}{2} L_h) + \frac{1}{k^2} L_h - P_5(\lambda, m) + \frac{i}{k} [P_4(\lambda, m) + P_3(\lambda, m)] + \\
 &\quad \frac{P_2(\lambda, m)}{k^2} [C(\lambda, m, k) + D(\lambda, m, k)] - \frac{i}{k^3} P_1(\lambda, m) D(k, \lambda, m)
 \end{aligned} \right\} \tag{B38}$$

2854

$$\begin{aligned}
 P_1(\lambda, m) &\equiv -\frac{2\varepsilon}{\pi^2 \lambda} I_1 \\
 P_2(\lambda, m) &\equiv -\frac{\varepsilon}{\pi^2 \lambda^2} I_2 \\
 P_3(\lambda, m) &\equiv -\frac{\varepsilon}{2\pi^2 \lambda^3} I_3 \\
 P_4(\lambda, m) &\equiv -\frac{\varepsilon}{4\pi^2 \lambda^3} I_4 \\
 P_5(\lambda, m) &\equiv -\frac{\varepsilon}{8\pi^2 \lambda^4} I_5 \\
 C(\lambda, m, k) &\equiv \frac{1 + ik + \frac{\varepsilon}{2\pi \lambda^2} k^2 e^{ik} I_7}{1 + i \frac{\varepsilon}{\lambda \pi} k e^{ik} I_6} \\
 D(\lambda, m, k) &\equiv -\frac{1 + ik - \frac{1}{2} k^2 - \frac{i\varepsilon}{8\pi \lambda^3} k^3 e^{ik} I_8}{1 + i \frac{\varepsilon}{\lambda \pi} k e^{ik} I_6}
 \end{aligned}
 \tag{B39}$$

and the I 's represent the following integrals:

$$\begin{aligned}
 I_1 &\equiv \int_{-1}^1 \frac{(\varepsilon+\eta)^{m-1}}{(\varepsilon-\eta)^m} \sqrt{\frac{1-\eta}{1+\eta}} \int_{-1}^1 \frac{(\varepsilon-\mu)^{m-1}}{(\varepsilon+\mu)^m} \sqrt{\frac{1+\mu}{1-\mu}} \frac{d\mu}{\eta-\mu} d\eta \\
 I_2 &\equiv \int_{-1}^1 \frac{(\varepsilon+\eta)^{m-1}}{(\varepsilon-\eta)^m} \sqrt{\frac{1-\eta}{1+\eta}} \int_{-1}^1 \frac{(\varepsilon-\mu)^{m-1}}{(\varepsilon+\mu)^m} \sqrt{\frac{1+\mu}{1-\mu}} \log \frac{\varepsilon+\mu}{\varepsilon-\mu} \frac{d\mu}{\eta-\mu} d\eta \\
 I_3 &\equiv \int_{-1}^1 \frac{(\varepsilon+\eta)^{m-1}}{(\varepsilon-\eta)^m} \sqrt{\frac{1-\eta}{1+\eta}} \log \frac{\varepsilon-\eta}{\varepsilon+\eta} \int_{-1}^1 \frac{(\varepsilon-\mu)^{m-1}}{(\varepsilon+\mu)^m} \sqrt{\frac{1+\mu}{1-\mu}} \log \frac{\varepsilon+\mu}{\varepsilon-\mu} \frac{d\mu}{\eta-\mu} d\eta \\
 I_4 &\equiv \int_{-1}^1 \frac{(\varepsilon+\eta)^{m-1}}{(\varepsilon-\eta)^m} \sqrt{\frac{1-\eta}{1+\eta}} \left(\log \frac{\varepsilon-\eta}{\varepsilon+\eta} \right)^2 \int_{-1}^1 \frac{(\varepsilon-\mu)^{m-1}}{(\varepsilon+\mu)^m} \sqrt{\frac{1+\mu}{1-\mu}} \frac{d\mu}{\eta-\mu} d\eta \\
 I_5 &\equiv \int_{-1}^1 \frac{(\varepsilon+\eta)^{m-1}}{(\varepsilon-\eta)^m} \sqrt{\frac{1-\eta}{1+\eta}} \left(\log \frac{\varepsilon-\eta}{\varepsilon+\eta} \right)^2 \int_{-1}^1 \frac{(\varepsilon-\mu)^{m-1}}{(\varepsilon+\mu)^m} \sqrt{\frac{1+\mu}{1-\mu}} \log \frac{\varepsilon+\mu}{\varepsilon-\mu} \frac{d\mu}{\eta-\mu} d\eta
 \end{aligned}
 \tag{B40}$$

2854

$$\begin{aligned}
 I_6 &\equiv \int_{-1}^1 \frac{(\epsilon+\eta)^{m-1}}{(\epsilon-\eta)^m} \sqrt{\frac{1-\eta}{1+\eta}} \int_1^\epsilon \frac{(\epsilon-\eta_1)^{\mu-1}}{(\epsilon+\eta_1)^\mu} \sqrt{\frac{\eta_1+1}{\eta_1-1}} \frac{d\eta_1}{\eta_1-\eta} d\eta \\
 I_7 &\equiv \int_{-1}^1 \frac{(\epsilon+\eta)^{m-1}}{(\epsilon-\eta)^m} \sqrt{\frac{1-\eta}{1+\eta}} \left(\log \frac{\epsilon-\eta}{\epsilon+\eta} \right) \int_1^\epsilon \frac{(\epsilon-\eta_1)^{\mu-1}}{(\epsilon+\eta_1)^\mu} \sqrt{\frac{\eta_1+1}{\eta_1-1}} \frac{d\eta_1}{\eta_1-\eta} d\eta \\
 I_8 &\equiv \int_{-1}^1 \frac{(\epsilon+\eta)^{m-1}}{(\epsilon-\eta)^m} \sqrt{\frac{1-\eta}{1+\eta}} \left(\log \frac{\epsilon-\eta}{\epsilon+\eta} \right)^2 \int_1^\epsilon \frac{(\epsilon-\eta_1)^{\mu-1}}{(\epsilon+\eta_1)^\mu} \sqrt{\frac{\eta_1+1}{\eta_1-1}} \frac{d\eta_1}{\eta_1-\eta} d\eta
 \end{aligned}
 \tag{B41}$$

It is to be noted in the preceding integrals that

$$\begin{aligned}
 |\epsilon| &\geq 1 & |\mu| &\leq 1 \\
 |\eta| &\leq 1 & |\eta_1| &\geq 1
 \end{aligned}$$

CQ-4

The integrals in equation (B40) are functions of only geometry and phasing between blades (λ and m). The P functions are therefore functions of geometry and phasing only. The integrals in equation (B41) are functions also of the reduced frequency k . The C and D functions are therefore functions of reduced frequency as well as of geometry and phasing. The integrals in equation (B40) are evaluated by integration around a closed contour in the complex plane. The details are given in appendix C. The integrals in equation (B41) are evaluated by means of the hypergeometric integral. The details are given in appendix D.

In the limiting case of the isolated airfoil ($\lambda = 0$), the following limiting values are obtained for the various functions:

$$\begin{aligned}
 \lambda \rightarrow 0 \quad P_1(\lambda, m) &\rightarrow 2 & P_2(\lambda, m) &\rightarrow 1 \\
 P_3(\lambda, m) &\rightarrow 0 & P_4(\lambda, m) &\rightarrow 1/2 & P_5(\lambda, m) &\rightarrow 1/8 \\
 C(\lambda, m, k) &\rightarrow C(k), \text{ Theodorsen's function} \\
 D(\lambda, m, k) &\rightarrow -C(k) - \frac{ik}{2} (1 - C(k)) + \frac{k^2}{4}
 \end{aligned}$$

Equations (B37) and (B38) then reduce to those for the isolated airfoil; L_h , L_α , M_h , and M_α reduce identically to the coefficients for the isolated airfoil given in reference 10.

2854

APPENDIX C

EVALUATION OF INTEGRALS I_1 TO I_5

The integrals I_1 to I_5 are evaluated by integrating around a closed contour in the complex ζ -plane, where the mapping function relating the η -plane to the ζ -plane is given by

$$\eta = \frac{1}{2}(\zeta + 1/\zeta) \tag{C1}$$

By use of equation (C1), equation (B40) can be written as double integrations around the closed contour C (fig. 7). Let

$$\begin{aligned} \zeta_1 &= \epsilon + \sqrt{\epsilon^2 - 1} & \zeta_2 &= \epsilon - \sqrt{\epsilon^2 - 1} = \frac{1}{\zeta_1} \\ \zeta_3 &= -\epsilon + \sqrt{\epsilon^2 - 1} = -\frac{1}{\zeta_1} & \zeta_4 &= -\epsilon - \sqrt{\epsilon^2 - 1} = -\zeta_1 \end{aligned}$$

Then

$$\begin{aligned} I_1 &= \frac{1}{2} \int_C \frac{(\zeta - \zeta_3)^{m-1} (\zeta - \zeta_4)^{m-1}}{(\zeta - \zeta_1)^m (\zeta - \zeta_2)^m} \frac{(\zeta - 1)^2}{\zeta} \int_C \frac{(\zeta' - \zeta_1)^{m-1} (\zeta' - \zeta_2)^{m-1}}{(\zeta' - \zeta_3)^m (\zeta' - \zeta_4)^m} \frac{(\zeta' + 1)^2}{(\zeta' - \zeta)(\zeta' - 1/\zeta)} d\zeta' d\zeta \\ I_2 &= \frac{1}{2} \int_C \frac{(\zeta - \zeta_3)^{m-1} (\zeta - \zeta_4)^{m-1}}{(\zeta - \zeta_1)^m (\zeta - \zeta_2)^m} \frac{(\zeta - 1)^2}{\zeta} \int_C \frac{(\zeta' - \zeta_1)^{m-1} (\zeta' - \zeta_2)^{m-1}}{(\zeta' - \zeta_3)^m (\zeta' - \zeta_4)^m} \frac{(\zeta' + 1)^2}{(\zeta' - \zeta)(\zeta' - 1/\zeta)} \log \frac{(\zeta' - \zeta_3)(\zeta' - \zeta_4)}{(\zeta_1 - \zeta')(\zeta' - \zeta_2)} d\zeta' d\zeta \\ I_3 &= \frac{1}{2} \int_C \frac{(\zeta - \zeta_3)^{m-1} (\zeta - \zeta_4)^{m-1}}{(\zeta - \zeta_1)^m (\zeta - \zeta_2)^m} \frac{(\zeta - 1)^2}{\zeta} \log \frac{(\zeta_1 - \zeta)(\zeta - \zeta_2)}{(\zeta - \zeta_3)(\zeta - \zeta_4)} \int_C \frac{(\zeta' - \zeta_1)^{m-1} (\zeta' - \zeta_2)^{m-1}}{(\zeta' - \zeta_3)^m (\zeta' - \zeta_4)^m} \frac{(\zeta' + 1)^2}{(\zeta' - \zeta)(\zeta' - 1/\zeta)} \log \frac{(\zeta' - \zeta_3)(\zeta' - \zeta_4)}{(\zeta_1 - \zeta')(\zeta' - \zeta_2)} d\zeta' d\zeta \\ I_4 &= \frac{1}{2} \int_C \frac{(\zeta - \zeta_3)^{m-1} (\zeta - \zeta_4)^{m-1}}{(\zeta - \zeta_1)^m (\zeta - \zeta_2)^m} \frac{(\zeta - 1)^2}{\zeta} \left[\log \frac{(\zeta_1 - \zeta)(\zeta - \zeta_2)}{(\zeta - \zeta_3)(\zeta - \zeta_4)} \right]^2 \int_C \frac{(\zeta' - \zeta_1)^{m-1} (\zeta' - \zeta_2)^{m-1}}{(\zeta' - \zeta_3)^m (\zeta' - \zeta_4)^m} \frac{(\zeta' + 1)^2}{(\zeta' - \zeta)(\zeta' - 1/\zeta)} d\zeta' d\zeta \\ I_5 &= \frac{1}{2} \int_C \frac{(\zeta - \zeta_3)^{m-1} (\zeta - \zeta_4)^{m-1}}{(\zeta - \zeta_1)^m (\zeta - \zeta_2)^m} \frac{(\zeta - 1)^2}{\zeta} \left[\log \frac{(\zeta_1 - \zeta)(\zeta - \zeta_2)}{(\zeta - \zeta_3)(\zeta - \zeta_4)} \right]^2 \int_C \frac{(\zeta' - \zeta_1)^{m-1} (\zeta' - \zeta_2)^{m-1}}{(\zeta' - \zeta_3)^m (\zeta' - \zeta_4)^m} \frac{(\zeta' + 1)^2}{(\zeta' - \zeta)(\zeta' - 1/\zeta)} \log \frac{(\zeta' - \zeta_3)(\zeta' - \zeta_4)}{(\zeta_1 - \zeta')(\zeta' - \zeta_2)} d\zeta' d\zeta \end{aligned} \tag{C2}$$

It is to be noted that in integrating around the closed contour C, the integration path C' in the η -plane is actually being traversed twice. Each integration around C must therefore be divided by 2.

If the integrations in (C2) are to be performed, the properties of the various integrands must be considered. It will suffice to discuss one of them, since they are all of the same general type.

2854

CQ-4 back

Consider the integral I_{31} defined by

$$I_{31} \equiv \int_C \frac{(\zeta' - \zeta_1)^{m-1} (\zeta' - \zeta_2)^{m-1}}{(\zeta' - \zeta_3)^m (\zeta' - \zeta_4)^m} \frac{(\zeta' + 1)^2}{(\zeta' - \zeta)(\zeta' - 1/\zeta)} \log \frac{(\zeta' - \zeta_3)(\zeta' - \zeta_4)}{(\zeta_1 - \zeta')(\zeta' - \zeta_2)} d\zeta' \quad (C3)$$

The integrand of I_{31} has branch points at ζ_1 , $\zeta_2 = 1/\zeta_1$, $\zeta_3 = -1/\zeta_1$, and $\zeta_4 = -\zeta_1$, as well as simple poles at ζ and $1/\zeta$. The transformation (C1) maps every point in the η -plane into a pair of reciprocal points in the ζ -plane. That part of C which lies below the real axis is therefore the reciprocal of that part of C which lies above the real axis, and every point which is outside the contour C has its reciprocal point inside the contour. The singularities of the integrand appear in reciprocal pairs, one of each pair lying outside the contour and one inside the contour. The poles at ζ and $1/\zeta$ lie on the contour (see fig. 7).

Considering the branch points, branch cuts are now made between ζ_2 and ζ_3 and from ζ_1 and ζ_4 to infinity as shown. The integrand is now unique and single-valued over the path of integration. Furthermore, it can readily be shown that since the integrand of I_{31} is invariant under the mapping $\zeta' \rightarrow 1/\zeta'$, (this evidently must be so because of (C1)), the sum of the residues at ζ and $1/\zeta$ must vanish identically. Consequently, any other contour such as C_0 , equivalent to C but excluding the points ζ and $1/\zeta$, may be used.

The integrand of I_{31} is therefore analytic in the annular region enclosed by the curves C_1 and C_2 as indicated in the figure. It can therefore be expanded into a Laurent series about the origin valid in this annular region. If A_{-1} is the coefficient of the $1/\zeta'$ term in this series, then

$$I_{31} = 2\pi i A_{-1} \quad (C4)$$

In order to expand the integrand into a Laurent series about the origin valid in the indicated annulus, equations (C2) will be written as follows:

$$\begin{aligned}
I_1 &= -\frac{1}{2\sigma^2} \int_0^1 \frac{\left(1 + \frac{1}{\sigma\zeta}\right)^{m-1} \left(1 + \frac{\zeta}{\sigma}\right)^{m-1}}{\left(1 - \frac{1}{\sigma\zeta}\right)^m \left(1 - \frac{\zeta}{\sigma}\right)^m} \left(1 - \frac{1}{\zeta}\right)^2 \int_0^1 \frac{\left(1 - \frac{1}{\sigma\zeta'}\right)^{m-1} \left(1 - \frac{\zeta'}{\sigma}\right)^{m-1}}{\left(1 + \frac{1}{\sigma\zeta'}\right)^m \left(1 + \frac{\zeta'}{\sigma}\right)^m} \frac{\frac{1}{\zeta'} (\zeta' + 1)^2}{\left(1 - \frac{\zeta'}{\zeta}\right) (1 - \zeta\zeta')} d\zeta' d\zeta \\
I_2 &= -\frac{1}{2\sigma^2} \int_0^1 \frac{\left(1 + \frac{1}{\sigma\zeta}\right)^{m-1} \left(1 + \frac{\zeta}{\sigma}\right)^{m-1}}{\left(1 - \frac{1}{\sigma\zeta}\right)^m \left(1 - \frac{\zeta}{\sigma}\right)^m} \left(1 - \frac{1}{\zeta}\right)^2 \int_0^1 \frac{\left(1 - \frac{1}{\sigma\zeta'}\right)^{m-1} \left(1 - \frac{\zeta'}{\sigma}\right)^{m-1}}{\left(1 + \frac{1}{\sigma\zeta'}\right)^m \left(1 + \frac{\zeta'}{\sigma}\right)^m} \left[\log \frac{\left(1 + \frac{1}{\sigma\zeta'}\right) \left(1 + \frac{\zeta'}{\sigma}\right)}{\left(1 - \frac{1}{\sigma\zeta'}\right) \left(1 - \frac{\zeta'}{\sigma}\right)} \right] \frac{\frac{1}{\zeta'} (\zeta' + 1)^2}{\left(1 - \frac{\zeta'}{\zeta}\right) (1 - \zeta\zeta')} d\zeta' d\zeta \\
I_3 &= -\frac{1}{2\sigma^2} \int_0^1 \frac{\left(1 + \frac{1}{\sigma\zeta}\right)^{m-1} \left(1 + \frac{\zeta}{\sigma}\right)^{m-1}}{\left(1 - \frac{1}{\sigma\zeta}\right)^m \left(1 - \frac{\zeta}{\sigma}\right)^m} \left[\log \frac{\left(1 - \frac{1}{\sigma\zeta}\right) \left(1 - \frac{\zeta}{\sigma}\right)}{\left(1 + \frac{1}{\sigma\zeta}\right) \left(1 + \frac{\zeta}{\sigma}\right)} \right] \left(1 - \frac{1}{\zeta}\right)^2 \int_0^1 \frac{\left(1 - \frac{1}{\sigma\zeta'}\right)^{m-1} \left(1 - \frac{\zeta'}{\sigma}\right)^{m-1}}{\left(1 + \frac{1}{\sigma\zeta'}\right)^m \left(1 + \frac{\zeta'}{\sigma}\right)^m} \left[\log \frac{\left(1 + \frac{1}{\sigma\zeta'}\right) \left(1 + \frac{\zeta'}{\sigma}\right)}{\left(1 - \frac{1}{\sigma\zeta'}\right) \left(1 - \frac{\zeta'}{\sigma}\right)} \right] \frac{\frac{1}{\zeta'} (\zeta' + 1)^2}{\left(1 - \frac{\zeta'}{\zeta}\right) (1 - \zeta\zeta')} d\zeta' d\zeta \\
I_4 &= -\frac{1}{2\sigma^2} \int_0^1 \frac{\left(1 + \frac{1}{\sigma\zeta}\right)^{m-1} \left(1 + \frac{\zeta}{\sigma}\right)^{m-1}}{\left(1 - \frac{1}{\sigma\zeta}\right)^m \left(1 - \frac{\zeta}{\sigma}\right)^m} \left[\log \frac{\left(1 - \frac{1}{\sigma\zeta}\right) \left(1 - \frac{\zeta}{\sigma}\right)}{\left(1 + \frac{1}{\sigma\zeta}\right) \left(1 + \frac{\zeta}{\sigma}\right)} \right]^2 \left(1 - \frac{1}{\zeta}\right)^2 \int_0^1 \frac{\left(1 - \frac{1}{\sigma\zeta'}\right)^{m-1} \left(1 - \frac{\zeta'}{\sigma}\right)^{m-1}}{\left(1 + \frac{1}{\sigma\zeta'}\right)^m \left(1 + \frac{\zeta'}{\sigma}\right)^m} \frac{\frac{1}{\zeta'} (\zeta' + 1)^2}{\left(1 - \frac{\zeta'}{\zeta}\right) (1 - \zeta\zeta')} d\zeta' d\zeta \\
I_5 &= -\frac{1}{2\sigma^2} \int_0^1 \frac{\left(1 + \frac{1}{\sigma\zeta}\right)^{m-1} \left(1 + \frac{\zeta}{\sigma}\right)^{m-1}}{\left(1 - \frac{1}{\sigma\zeta}\right)^m \left(1 - \frac{\zeta}{\sigma}\right)^m} \left[\log \frac{\left(1 - \frac{1}{\sigma\zeta}\right) \left(1 - \frac{\zeta}{\sigma}\right)}{\left(1 + \frac{1}{\sigma\zeta}\right) \left(1 + \frac{\zeta}{\sigma}\right)} \right]^2 \left(1 - \frac{1}{\zeta}\right)^2 \int_0^1 \frac{\left(1 - \frac{1}{\sigma\zeta'}\right)^{m-1} \left(1 - \frac{\zeta'}{\sigma}\right)^{m-1}}{\left(1 + \frac{1}{\sigma\zeta'}\right)^m \left(1 + \frac{\zeta'}{\sigma}\right)^m} \left[\log \frac{\left(1 + \frac{1}{\sigma\zeta'}\right) \left(1 + \frac{\zeta'}{\sigma}\right)}{\left(1 - \frac{1}{\sigma\zeta'}\right) \left(1 - \frac{\zeta'}{\sigma}\right)} \right] \frac{\frac{1}{\zeta'} (\zeta' + 1)^2}{\left(1 - \frac{\zeta'}{\zeta}\right) (1 - \zeta\zeta')} d\zeta' d\zeta
\end{aligned}$$

(c5)

where

$$\sigma \equiv \zeta_1 = \frac{1}{\zeta_2} = -\frac{1}{\zeta_3} = -\zeta_4 = \varepsilon + \sqrt{\varepsilon^2 - 1} = \coth \frac{\lambda}{2}$$

Each integrand can now be obtained in the form of a Laurent series about the origin by expanding each bracketed quantity (noting that each of these series will converge at least within the annulus) and multiplying the resultant series together. In this way, for example, the coefficient of $1/\zeta'$ can be obtained and the inner integration performed. This coefficient will, in general, be an infinite series in ζ . The process then has to be repeated to carry out the second integration. The final result will be a doubly or triply infinite series in σ . The process is evidently extremely long and laborious. However, it can be greatly simplified by employing a set of recurrence formulas which can be obtained by inspection of the series, whereby each term of a given infinite series is obtained in terms of a previously given series. The calculation scheme is as follows: Let

$$a_0 = 0; a_1 = 1; b_0 = 1$$

$$a_{j+1} = \frac{1}{j} [(j-2)a_{j-1} - 2ma_j]$$

$$b_j = b_{j-1} + a_{j+1}$$

$$c_j = \sigma^{-j} \sum_{i=0}^{\infty} \frac{b_i b_{i+j}}{\sigma^{2i}} = c_{-j}$$

$$d_j = \sum_{i=0}^{\infty} \frac{c_{j+1+2i} + c_{j-1-2i}}{(2i+1)\sigma^{2i}} = d_{-j}$$

$$e_j = \sum_{i=0}^{\infty} \frac{d_{j+1+2i} + d_{j-1-2i}}{(2i+1)\sigma^{2i}} = e_{-j}$$

$$C_j = (-1)^j (c_{j-1} + 2c_j + c_{j+1}) \left(c_j + 2 \sum_{i=j}^{\infty} c_{i+1} \right)$$

$$D_j = (-1)^j (d_{j-1} + 2d_j + d_{j+1}) \left(c_j + 2 \sum_{i=j}^{\infty} c_{i+1} \right)$$

$$E_j = (-1)^j (e_{j-1} + 2e_j + e_{j+1}) \left(c_j + 2 \sum_{i=j}^{\infty} c_{i+1} \right)$$

$$F_j = (-1)^j (d_{j-1} + 2d_j + d_{j+1}) \sum_{i=0}^{j-1} (d_{j-2i} + d_{j-1-2i})$$

$$G_j = (-1)^j (d_{j-1} + 2d_j + d_{j+1}) \sum_{i=0}^{j-1} (e_{j-2i} + e_{j-1-2i})$$

Then:

$$I_1 = -\frac{4\pi^2}{\sigma^2} \left(\frac{1}{2} C_0 + \sum_{j=1}^{\infty} C_j \right)$$

$$I_2 = -\frac{8\pi^2}{\sigma^3} \left(\frac{1}{2} D_0 + \sum_{j=1}^{\infty} D_j \right)$$

$$I_3 = \frac{16\pi^2}{\sigma^4} \sum_{j=1}^{\infty} F_j$$

$$I_4 = -\frac{16\pi^2}{\sigma^4} \left(\frac{1}{2} E_0 + \sum_{j=1}^{\infty} E_j \right)$$

$$I_5 = \frac{32\pi^2}{\sigma^5} \sum_{j=1}^{\infty} G_j$$

APPENDIX D

EVALUATION OF INTEGRALS I_6 TO I_8

Let

$$v \equiv \frac{1}{T} \left(1 - \tau^{-1/2} \frac{\varepsilon - \eta}{\varepsilon + \eta} \right)$$

$$v_1 \equiv \tau^{1/2} \frac{\varepsilon - \eta_1}{\varepsilon + \eta_1} \quad (D1)$$

$$\tau^{1/2} \equiv \frac{\varepsilon + 1}{\varepsilon - 1}$$

$$T \equiv \frac{\tau - 1}{\tau}$$

$$T' \equiv \frac{\tau - 1}{\tau - v_1}$$

The order of integration is reversed and the logs are expanded in order that equations (B4) can be written as follows:

$$I_6 = \frac{T \tau}{2\varepsilon} \int_0^1 v_1^{\kappa-1} (1-v_1)^{-1/2} \left(1 - \frac{v_1}{\tau} \right)^{-1/2} \int_0^1 v^{-1/2} (1-v)^{1/2} (1-Tv)^{-m} (1-T'v)^{-1} dv dv_1$$

$$I_7 = - \frac{T \tau}{2\varepsilon} \sum_{j=1}^{\infty} \frac{T^j}{j} \int_0^1 v_1^{\kappa-1} (1-v_1)^{-1/2} \left(1 - \frac{v_1}{\tau} \right)^{-1/2} \int_0^1 v^{j-1/2} (1-v)^{1/2} (1-Tv)^{-m} (1-T'v)^{-1} dv dv_1 + \frac{1}{2} I_6 \log \tau$$

$$I_8 = \frac{T \tau}{2\varepsilon} \sum_{i=1}^{\infty} \sum_{j=1}^{\infty} \frac{T^{i+j}}{ij} \int_0^1 v_1^{\kappa-1} (1-v_1)^{-1/2} \left(1 - \frac{v_1}{\tau} \right)^{-1/2} \int_0^1 v^{i+j-1/2} (1-v)^{1/2} (1-Tv)^{-m} (1-T'v)^{-1} dv dv_1 + I_7 \log \tau - \frac{1}{4} I_6 \log^2 \tau \quad (D2)$$

The inner integral is the same for all three, except for the exponent of v . This integral can be evaluated in terms of Appell's hypergeometric function in two variables of the first kind (refs. 16 and 17).

$$\int_0^1 v^{n-1/2} (1-v)^{1/2} (1-Tv)^{-m} (1-T'v)^{-1} dv = \frac{\Gamma(n+1/2)\Gamma(3/2)}{\Gamma(n+2)}$$

$$F_1(n+1/2; m, 1; n+2; T, T') \tag{D3}$$

$\Gamma(n)$ Gamma function of argument n .

The hypergeometric function F_1 is defined in terms of a double infinite sum in T and T' .

$$F_1(n+1/2; m, 1; n+2; T, T') = \sum_{p=0}^{\infty} \sum_{q=0}^{\infty} \frac{(n+1/2, p+q)(m, p)}{(n+2, p+q)p!} T^p (T')^q \tag{D4}$$

where

$$(n, p) \equiv n(n+1)(n+2) \cdots (n+p-1) = \frac{\Gamma(n+p)}{\Gamma(n)} \tag{D5}$$

$$(n, 0) \equiv 1; (1, n) = n!$$

F_1 can also be expressed as a single infinite sum of ordinary hypergeometric functions.

$$F_1(n+1/2; m, 1; n+2; T, T') = \sum_{k=0}^{\infty} \frac{(n+1/2, p)(1+m, p)}{(n+2, p)p!} T^p F\left(-p, 1; 1+m; 1 - \frac{T'}{T}\right) \tag{D6}$$

where $F\left(-p, 1; 1+m; 1 - \frac{T'}{T}\right)$ is a polynomial given by

$$\begin{aligned} F\left(-p, 1; 1+m; 1 - \frac{T'}{T}\right) &= \sum_{q=0}^p \frac{(-p, q)}{(1+m, q)} \left(1 - \frac{T'}{T}\right)^q \\ &= \sum_{q=0}^p (-)^q \tau^{-q} \frac{(-p, q)}{(1+m, q)} v_1^q \left(1 - \frac{v_1}{\tau}\right)^{-q} \end{aligned} \tag{D7}$$

2854

5-00

Upon substituting back into equations (D2), the following integral remains to be evaluated:

$$\int_0^1 v_1^{\kappa-1+q} (1-v_1)^{-1/2} \left(1 - \frac{v_1}{\tau}\right)^{-1/2-q} dv$$

$$= \frac{\Gamma(\kappa+q)\Gamma(1/2)}{\Gamma(\kappa+q+1/2)} F(q+1/2, \kappa+q; \kappa+q+1/2; 1/\tau) \quad (D8)$$

$$= \frac{\Gamma(\kappa+q)\Gamma(1/2)}{\Gamma(\kappa+q+1/2)} T^{-q} F(1/2, \kappa; \kappa+1/2+q; 1/\tau)$$

2854

(ref. 18)

Equations (D2) can now be written as follows:

$$I_6 = \pi \frac{T \tau^{\frac{1-\kappa-m}{2}}}{4\epsilon} \frac{\Gamma(\kappa)\Gamma(1/2)}{\Gamma(\kappa+1/2)} \sum_{p=0}^{\infty} A_p B_p T^p$$

$$I_7 = -\pi \frac{T \tau^{\frac{1-\kappa-m}{2}}}{4\epsilon} \frac{\Gamma(\kappa)\Gamma(1/2)}{\Gamma(\kappa+1/2)} \sum_{j=1}^{\infty} \sum_{p=0}^{\infty} \frac{1}{j} A_{j+p} B_p T^{j+p} + 2\lambda I_6$$

$$I_8 = \pi \frac{T \tau^{\frac{1-\kappa-m}{2}}}{4\epsilon} \frac{\Gamma(\kappa)\Gamma(1/2)}{\Gamma(\kappa+1/2)} \sum_{i=1}^{\infty} \sum_{j=1}^{\infty} \sum_{p=0}^{\infty} \frac{1}{ij} A_{i+j+p} B_p T^{i+j+p} - 4\lambda^2 I_6 + 4\lambda I_7$$

(D9)

where

$$A_{i+j+p} \equiv \frac{\Gamma(i+j+p+1/2)}{\Gamma(i+j+p+2)\Gamma(1/2)}$$

with

$$A_0 = 1$$

and

$$A_{i+j+p+1} = \frac{i+j+p+1/2}{i+j+p+2} A_{i+j+p}$$

$$B_p = \frac{(1+m, p)}{p!} \sum_{q=0}^p (-1)^q \frac{(\lambda, q)(-p, q)}{(\lambda+1/2, q)(1+m, q)} (\tau T)^{-q} F(1/2, \lambda; \lambda+1/2+q; 1/\tau) \tag{D10}$$

Let:

$$R_1 \equiv 1 + \frac{\lambda-m}{2} T \tau^{1/2-m} \frac{\Gamma(\lambda)\Gamma(1/2)}{\Gamma(\lambda+1/2)} \sum_{p=0}^{\infty} A_p B_p T^p$$

$$R_2 \equiv 1 + \frac{(\lambda-m)^2}{2} T \tau^{1/2-m} \frac{\Gamma(\lambda)\Gamma(1/2)}{\Gamma(\lambda+1/2)} \sum_{j=1}^{\infty} \sum_{p=0}^{\infty} \frac{1}{j} A_{j+p} B_p T^{j+p}$$

$$R_3 \equiv 1 + \frac{(\lambda-m)^3}{4} T \tau^{1/2-m} \frac{\Gamma(\lambda)\Gamma(1/2)}{\Gamma(\lambda+1/2)} \sum_{i=1}^{\infty} \sum_{j=1}^{\infty} \sum_{p=0}^{\infty} \frac{1}{ij} A_{i+j+p} B_p T^{i+j+p} \tag{D11}$$

Then equations (B38) for C and D can be written as follows:

$$C(\lambda, m, k) = -ik + \frac{2ik + R_2}{R_1} \tag{D12}$$

$$D = ik C - \frac{k^2}{2} - \frac{2ik - 2k^2 + R_3}{R_1}$$

2854

back 5-00

REFERENCES

1. Mendelson, Alexander: Effect of Centrifugal Force on Flutter of Uniform Cantilever Beam at Subsonic Speeds with Application to Compressor and Turbine Blades. NACA TN 1893, 1949.
2. Halfman, Robert L., Johnson, H. C., and Haley, S. M.: Evaluation of High-Angle-of-Attack Aerodynamic-Derivative Data and Stall-Flutter Prediction Techniques. NACA TN 2533, 1951.
3. Mendelson, Alexander: Effect of Aerodynamic Hysteresis on Critical Flutter Speed at Stall. NACA RM E8B04, 1948. (See also Jour. Aero. Sci., vol. 16, no. 11, Nov. 1949, pp. 645-654.)
4. Reissner, E.: Wind Tunnel Corrections for the Two-Dimensional Theory of Oscillating Airfoils. Aero-Mech. Dept., Rep. No. SB-318-S-3, Cornell Aero. Lab., Inc., Apr. 22, 1947.
5. Timman, R.: The Aerodynamic Forces on an Oscillating Aerofoil Between Two Parallel Walls. Appl. Sci. Res., vol. A3, no. 1, 1951, pp. 31-57.
6. Lilley, G. M.: An Investigation of the Flexure-Torsion Flutter Characteristics of Aerofoils in Cascade. Rep. No. 60, The College of Aero. (Cranfield), May 1952.
7. Billington, A. E.: Aerodynamic Lift and Moment for Oscillating Aerofoils in Cascade. Rep. E.63, Div. Aero., Council of Sci. and Ind. Res., Jan. 1, 1949.
8. Theodorsen, Theodore: General Theory of Aerodynamic Instability and the Mechanism of Flutter. NACA Rep. 496, 1935.
9. Sisto, F.: Flutter of Airfoils in Cascade. Sc. D. Thesis, M.I.T., Sept. 1952.
10. Smilg, Benjamin, and Wasserman, L. S.: Application of Three-Dimensional Flutter Theory to Aircraft Structures. Army Air Forces Tech. Rep. No. 4798, War Dept., Army Air Forces, Materiel Center, Wright Field, Dayton (Ohio), July 8, 1942.
11. Sisto, Fernando: Stall Flutter in Cascades. Preprint No. 402, Inst. Aero. Sci., 1953.
12. Bromwich, T. J. I'a: An Introduction to the Theory of Infinite Series. Macmillan and Co., Ltd. (London), 1942.

13. Betz, A.: Tragflügeltheorie. Ber. und Abh. der Wiss. Gesellschaft für Luftfahrt, Bd. 1, Heft 2, Oct. 1920.
14. Schröder, Kurt: Über eine Integralgleichung erster Art der Tragflügeltheorie. Akad. der Wiss. (Berlin), Sitz. der phys. - Math. Klasse, 1938, pp. 345-362.
15. Sohngen, Heinz: Die Lösungen der Integralgleichung $g(x) = \frac{1}{2\pi} \int_{-a}^a \frac{f(\xi)}{x-\xi} d\xi$ und deren Anwendung in der Tragflügeltheorie. Math. Zs., Bd. 15, 1939, pp. 245-264.
16. Appell, P., and Kampé de Fériet, J.: Fonctions Hypergéométriques et Hypersphériques - Polynomes d'Hermite. Gauthier-Villars, Paris, 1926.
17. Whittaker, E. T., and Watson, G. N.: A Course of Modern Analysis. Cambridge Univ. Press, 1952.
18. Snow, Chester: The Hypergeometric and Legendre Functions with Applications to Integral Equations of Potential Theory. Dept. Commerce, Nat. Bur. Standards, 1942.

TABLE I. - GEOMETRIC PARAMETERS

$$\left[\lambda = \frac{\pi}{s}, \epsilon = \coth \lambda, \tau = \left(\frac{\epsilon+1}{\epsilon-1} \right)^2, T = \frac{\tau-1}{\tau}, \sigma = \coth \frac{\lambda}{2} \right]$$

s	λ	ϵ	σ	$\tau \times 10^{-3}$	T
1.0	3.1416	1.0037	1.0903	293.27	1.0000
1.1	2.8560	1.0066	1.1220	92.434	1.0000
1.2	2.6180	1.0107	1.1573	35.312	1.0000
1.3	2.4166	1.0160	1.1959	15.876	.9999
1.4	2.2440	1.0227	1.2372	7.9398	.9999
1.5	2.0944	1.0308	1.2809	4.3474	.9998
1.6	1.9635	1.0402	1.3265	2.5757	.9996
1.7	1.8480	1.0509	1.3740	1.6235	.9994
1.8	1.7453	1.0629	1.4231	1.0756	.9991
1.9	1.6535	1.0760	1.4733	.74615	.9987
2.0	1.5708	1.0903	1.5249	.53585	.9981
2.1	1.4960	1.1057	1.5774	.39687	.9975
2.2	1.4280	1.1220	1.6308	.30253	.9967
2.3	1.3659	1.1393	1.6850	.23585	.9958
2.4	1.3090	1.1574	1.7401	.18787	.9947
2.5	1.2566	1.1763	1.7957	.15238	.9934
2.6	1.2083	1.1959	1.8517	.12565	.9920
2.7	1.1636	1.2162	1.9085	.10508	.9905
2.8	1.1220	1.2372	1.9657	.088957	.9888
2.9	1.0833	1.2588	2.0235	.076178	.9869
3.0	1.0472	1.2809	2.0813	.065934	.9848
3.2	.9817	1.3266	2.1985	.050747	.9803
3.4	.9240	1.3740	2.3164	.040292	.9752
3.6	.8727	1.4230	2.4351	.032811	.9695
3.8	.8267	1.4734	2.5552	.027299	.9634
4.0	.7854	1.5249	2.6760	.023138	.9568
5.0	.6283	1.7957	3.2867	.012345	.9190
•	-----	-----	-----	-----	-----

2854

TABLE II. - b_j COEFFICIENTS

j	b_j		j	b_j	
	m=0	m=1/2		m=0	m=1/2
0	1	1	11	1	0
1	1	0	12	1	.2256
2	1	.5	13	1	0
3	1	0	14	1	.2095
4	1	.375	15	1	0
5	1	0	16	1	.1964
6	1	.3125	17	1	0
7	1	0	18	1	.1855
8	1	.2734	19	1	0
9	1	0	20	1	.1762
10	1	.2461			

TABLE III. - A_j COEFFICIENTS

j	A_j	j	A_j
0	1	16	0.008232
1	.2500	17	.007546
2	.1250	18	.006950
3	.07812	19	.006429
4	.05468	20	.005970
5	.04101	21	.005563
6	.03222	22	.005200
7	.02618	23	.004875
8	.02182	24	.004582
9	.01855	25	.004318
10	.01602	26	.004078
11	.01402	27	.003860
12	.01240	28	.003660
13	.01107	29	.003477
14	.009963	30	.003309
15	.009029		

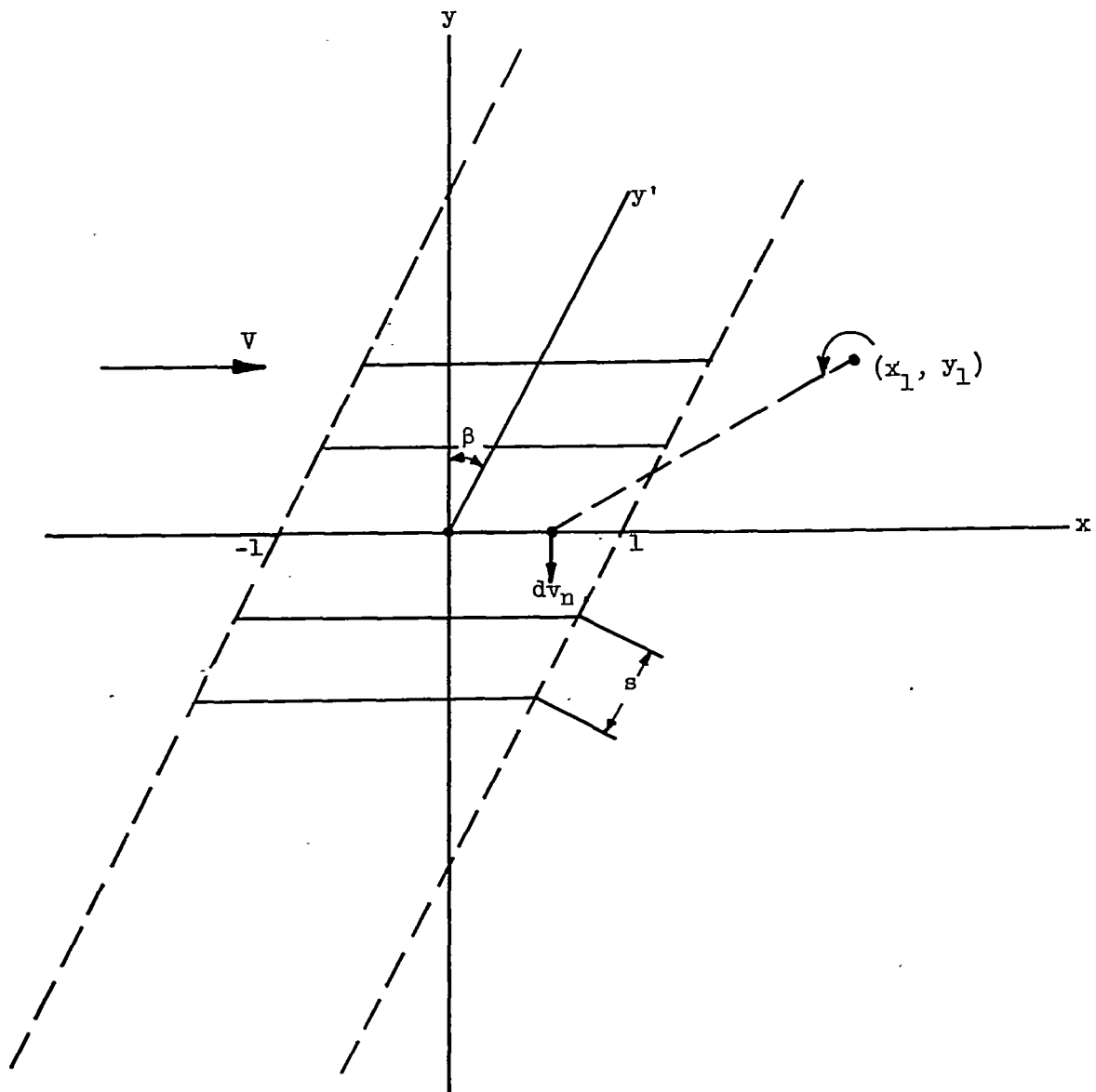


Figure 1. - Cascade geometry.

2854

CQ-6

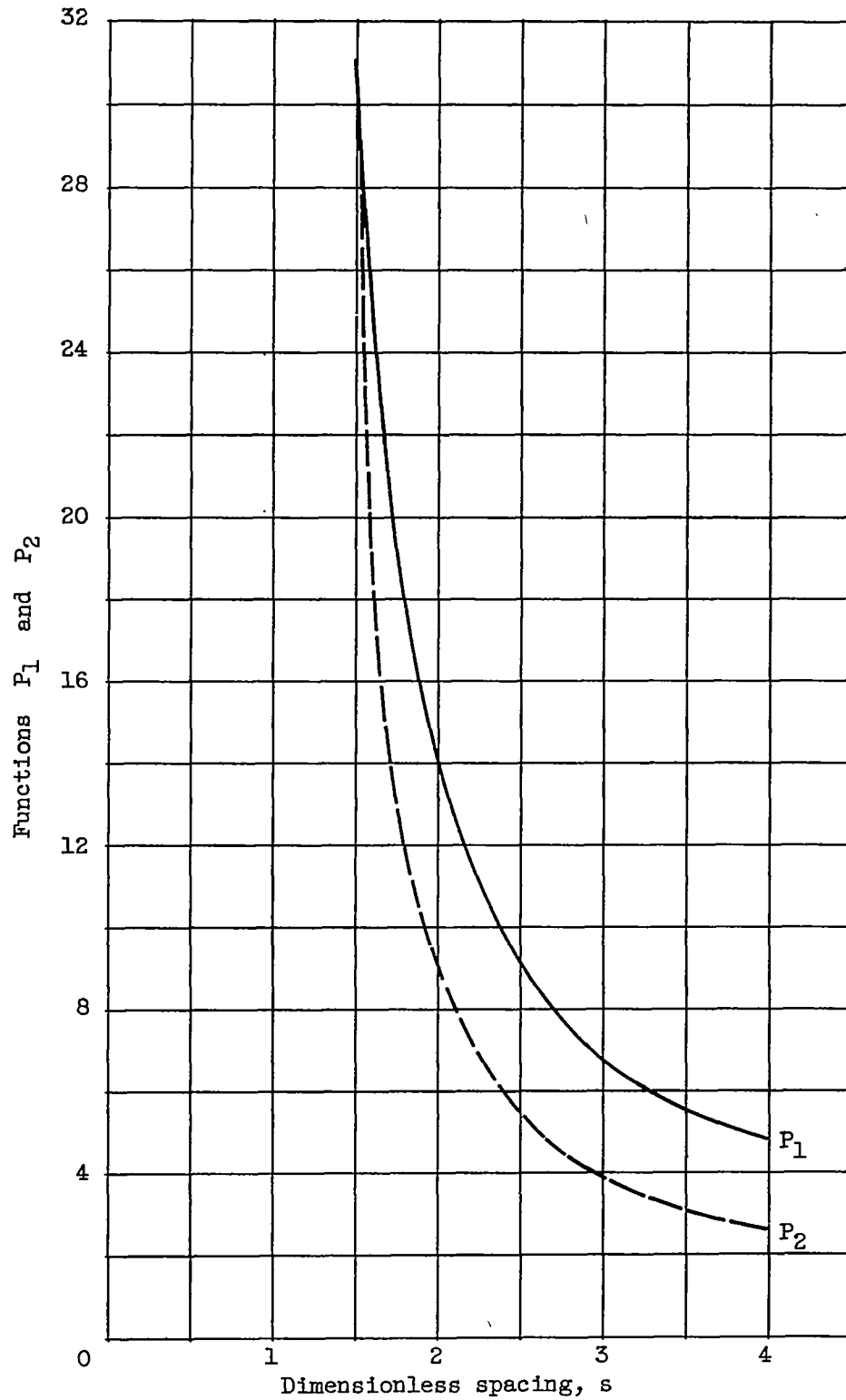


Figure 2. - Variation of P_1 and P_2 with spacing.

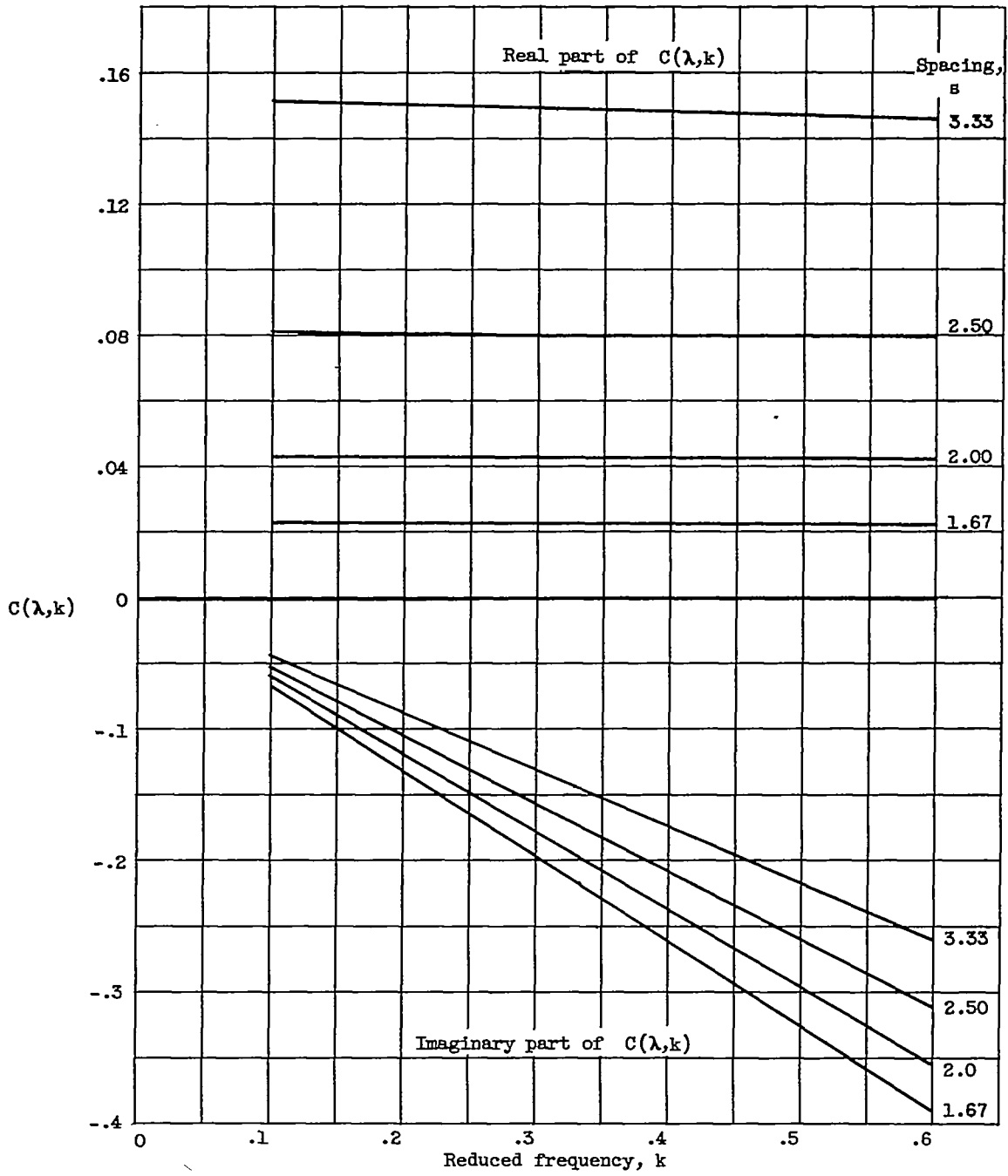


Figure 3. - Variation of real and imaginary parts of $C(\lambda, k)$ with reduced frequency k for various values of spacing s . Phase lag m , 0.

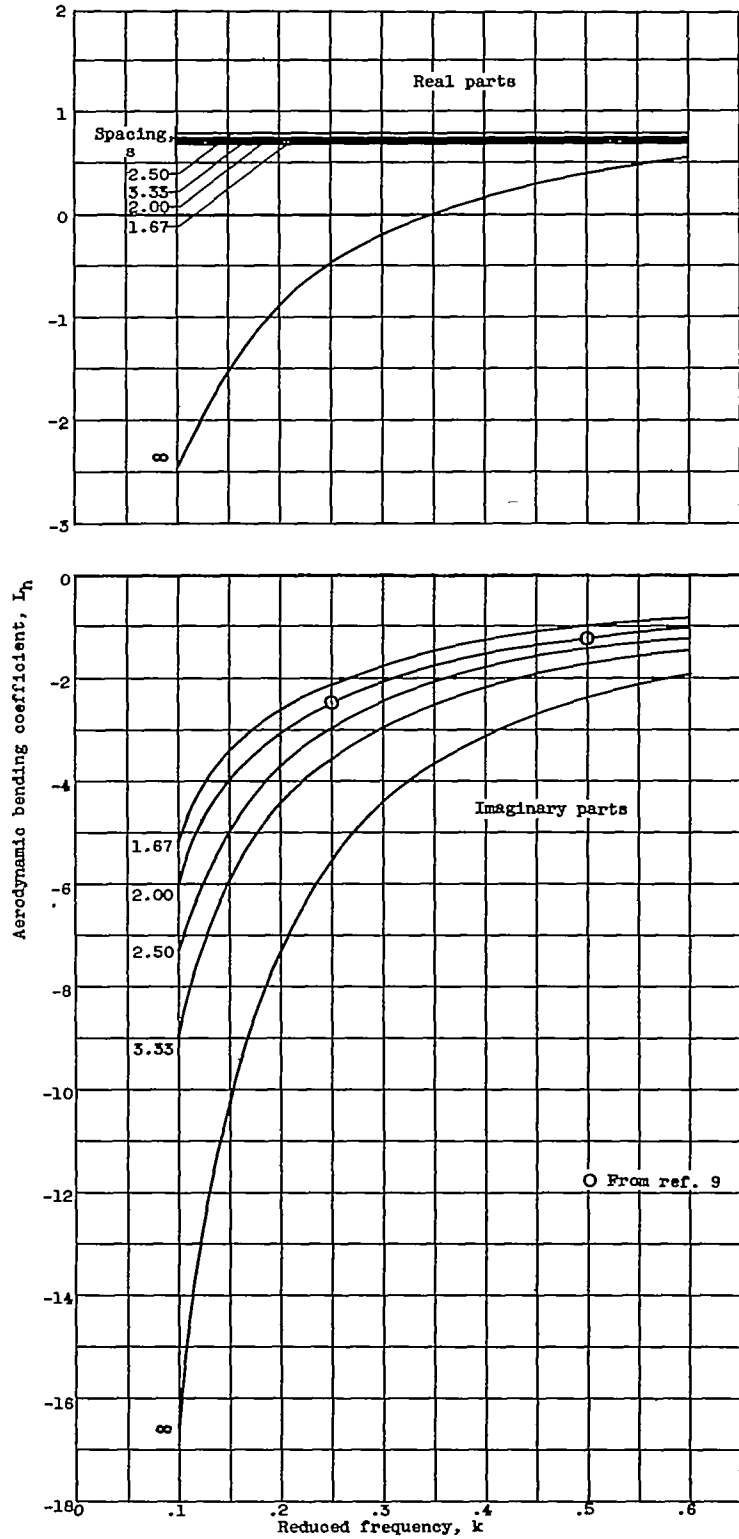


Figure 4. - Variation of bending coefficient L_n with reduced frequency k for various values of spacing s , Phase lag, 0.

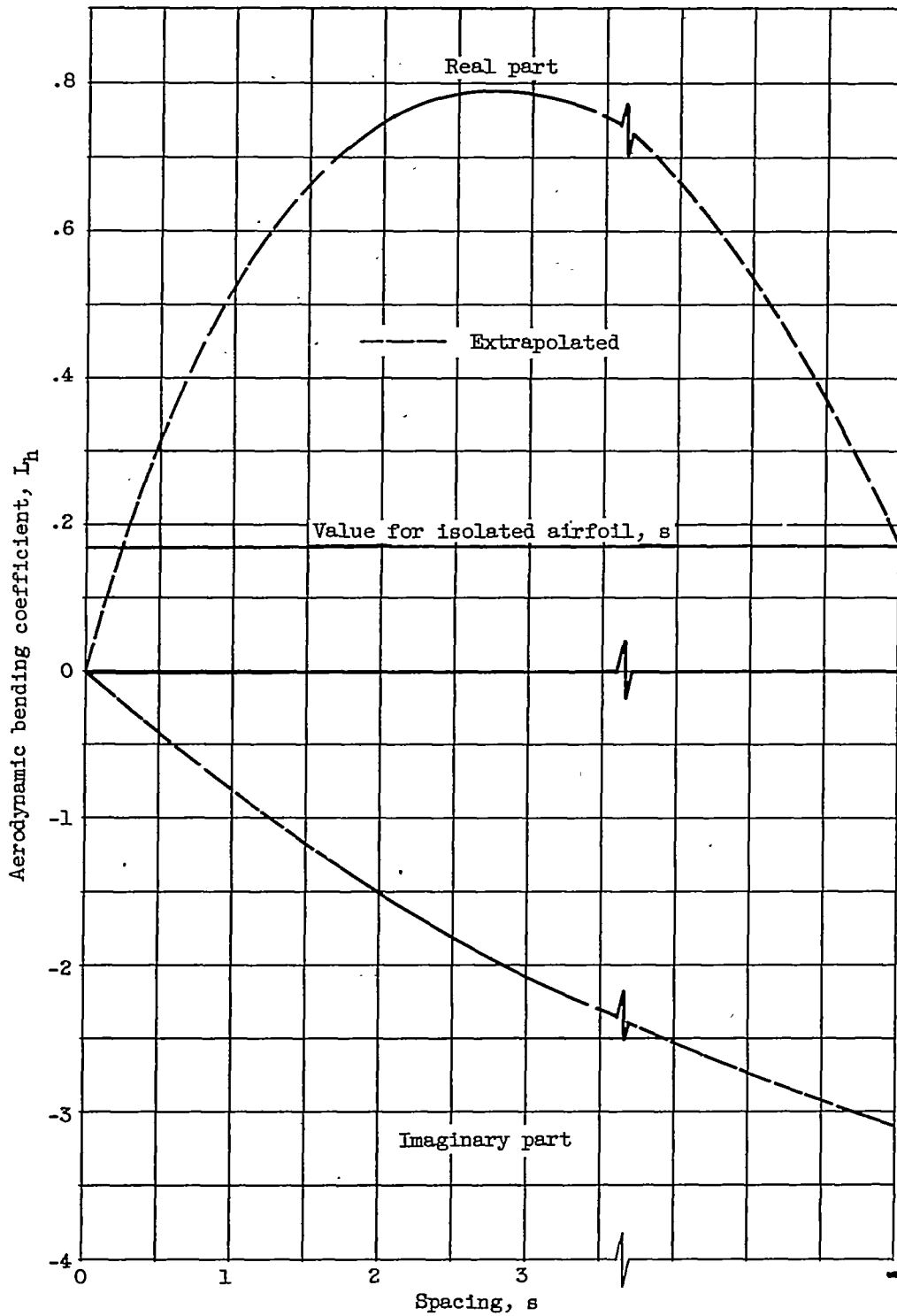


Figure 5. - Variation of bending coefficient L_h with spacing s .
Reduced frequency, 0.4; phase lag m , 0.

2854

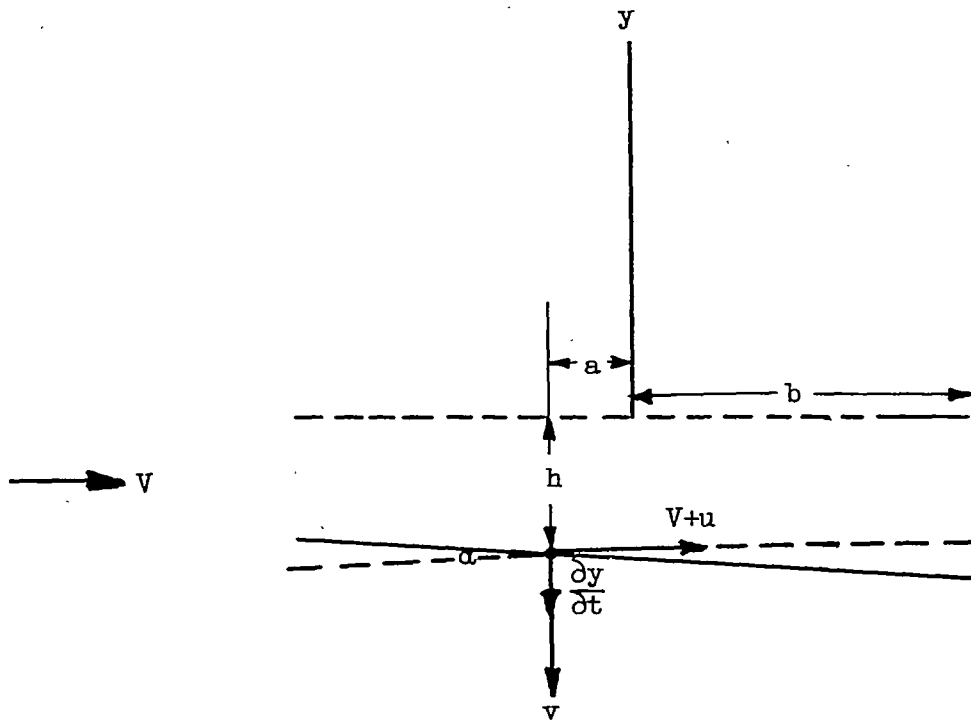


Figure 6. - Airfoil displacements.

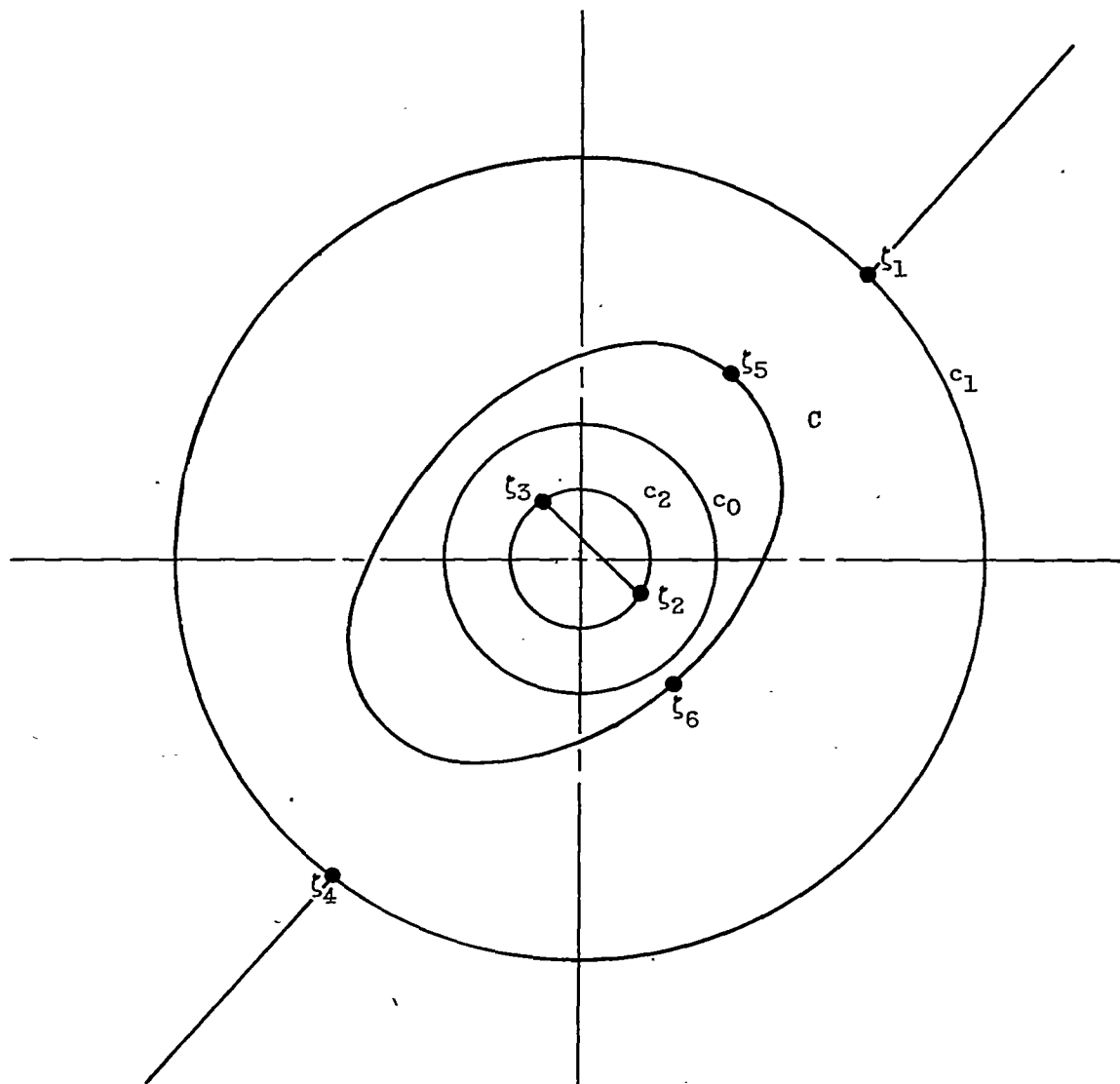


Figure 7. - Contours in ζ -plane.